Assimilation of precipitation information at ECMWF

Peter Bauer[1], Philippe Lopez, Emmanuel Moreau, Angela Benedetti,
Adrian Tompkins, Marta Janiskovà
ECMWF, Reading, UK

Humidity analysis represents a large challenge for numerical weather prediction because the accuracy of the representation of the hydrological cycle in a global model depends on the accuracy and representativeness of physical parameterizations. These have to cover the response of the atmospheric moisture fields to large-scale dynamics, cloud and precipitation formation and fluxes at the surface atmosphere boundary. Beljaars (2003) assesses the ECMWF model performance with respect to the atmospheric moisture representation. The main conclusions are that too much precipitation is generated over the entire dynamic range of rain rates but that the model has a dry bias outside areas with precipitation. The precipitation-bias and its reflection in total column water vapour (TCWV) was confirmed by Marécal et al. (2002) when comparing near-surface rain estimates from satellite data and model fields as well as the atmospheric moisture required for producing the respective rainfall intensities. The clear-sky dry bias has been noted at least since the assimilation of satellite data that is almost entirely sensitive to the TCWV (Gerard and Saunders 1999) and its manifestation in the so-called tropical precipitation spin-down that is the overproduction of rain originating from the moistening of the atmosphere in the analysis. This, of course, feeds back into the large-scale dynamics through the release of latent heat.

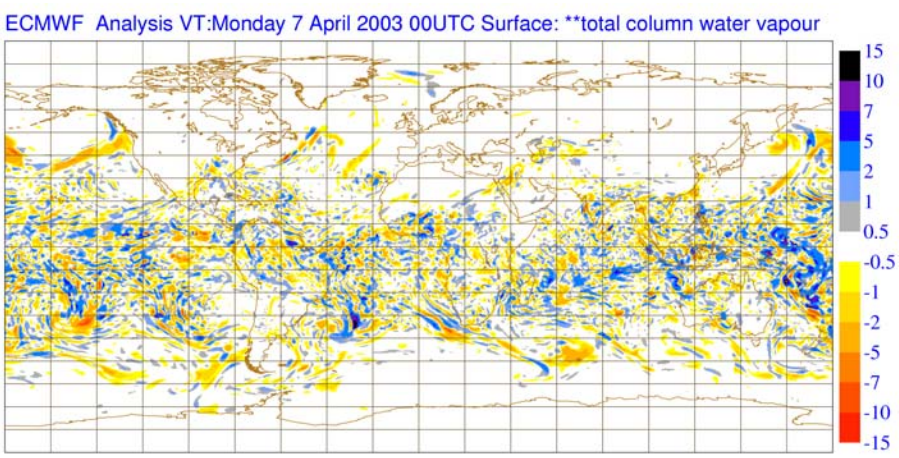

Figure 1: Difference of humidity increments between rain assimilation and control experiment (kg/m2).

Apart from improved physical parameterizations, the inclusion of observations directly related to clouds and precipitation will improve the humidity analysis - an effect that may dissipate during the forecast. At ECMWF, large efforts have been made for almost five years to prepare the assimilation of precipitation information. Marécal and Mahfouf (2000, 2002) have laid the foundation for the methodology that is likely to become operational in 2004. TCWV in rain-affected areas is estimated by a one-dimensional variational retrieval (1D-Var) that uses retrieved rain rates or microwave radiances (Moreau et al. 2003a) as observations. These TCWV 'pseudo-observations' are then assimilated like other observations in the 4D-Var system.

The intermediate 1D-Var protects the incremental 4D-Var assimilation from the strongly non-linear response of cloud and convection schemes to moisture increments as well as from the

[1] peter.bauer@ecmwf.int

(weakly) non-linear relationship between radiances and water vapour / condensate (Marécal and Mahfouf 2003, Moreau et al. 2003b). All these developments required updated cloud (Tompkins and Janiskovà 2003) and convection (Lopez and Moreau 2003) schemes as well as their linearized versions in the minimization. Figure 1 shows an example of TCWV analysis increments from assimilating rain observations on April 7, 2003. While the global hydrological budget remains nearly unchanged there are large local increments that can be mainly associated with the displacement of precipitating systems. The effect of the assimilation of satellite data only between 40S-40N spreads to higher latitudes with similar increment values as observed in the Tropics. Figure 2 shows the improvement of the forecasted track of hurricane Isabel on September 15, 2003, computed from the analysis at 12 UTC.

Sensitivity studies indicate that the storm-track prediction quality highly depends on the combined effect of different observation types on humidity and dynamics. Therefore a thorough data screening is crucial for optimizing both analysis and forecast as a function of observational data and the representation of clouds and precipitation through physical parameterizations. In any case, the four-dimensional variational data assimilation system that is operated at ECMWF provides a very flexible framework for the improvement of the humidity analysis near precipitating systems.

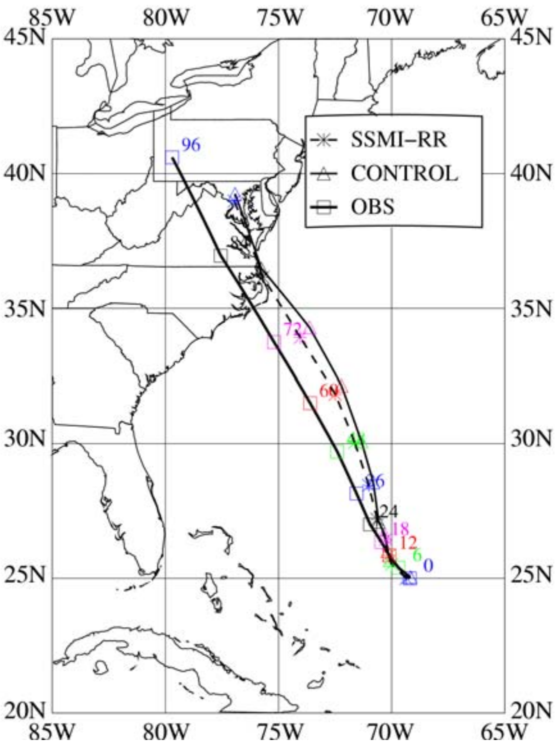

Figure 2: Hurricane Isabel track forecast on 2003/09/15.

References

Beljaars, A., 2003: Some aspects of modelling of the hydrological cycle in the ECMWF model. Proceedings of ECMWF/GEWEX Workshop on Humidity Analysis, 8-11 July 2002, ECMWF, Reading, UK, 191-202.

Gerard, E. and R. Saunders, 1999: Four-dimensional variational assimilation of Special Sensor Microwave / Imager total column water vapour in the ECMWF model. *Q.J.R. Meteorol. Soc.*, **125**, 1453-1468.

Lopez, P. and E. Moreau, 2003: A convection scheme for data assimilation: Description and initial tests. Technical report. ECMWF Technical Memorandum No. 411, in press.

Marécal, V. and J.-F. Mahfouf, 2000: Variational retrieval of temperature and humidity profiles from TRMM precipitation data. *Mon. Weather Rev.*, **128**, 3853-3866.

Marécal, V., J.-F. Mahfouf, and P. Bauer, 2002: Comparison of TMI rainfall estimates and their impact on 4D-Var assimilation. *Q. J. R. Meteorol. Soc.*, **128**, 2737-2758.

Marécal, V. and J.-F. Mahfouf, 2003: Experiments on 4D-Var assimilation of rainfall data using an incremental formulation. *Q. J. R. Meteorol. Soc.*, **128**, 2737-2758.

Moreau, E., P. Bauer, and F. Chevallier, 2003a: Variational retrieval of rain profiles from spaceborne passive microwave radiance observations. *J. Geophys. Res.*, **108**, ACL 11-1 - 11-18.

Moreau, E., P. Lopez, P. Bauer, A. Tompkins, M. Janiskovà and F. Chevallier, 2003b: Variational retrieval of temperature and humidity profiles using rain-rates versus microwave brightness temperatures. *Q. J. R. Meteorol. Soc.*, submitted.

Tompkins, A.and M. Janiskovà, 2003: A cloud scheme for data assimilation: Description and initial tests. *Q. J. R. Meteorol. Soc.*, submitted.

VARIATIONAL DATA ASSIMILATION AT THE ITALIAN AIR FORCE WEATHER SERVICE: A PROGRESS REPORT

Massimo Bonavita & Lucio Torrisi
CNMCA, Italian Air Force Weather Service, Pratica di Mare, Rome

Development and Implementation of CNMCA 3D-PSAS Assimilation System

A new data assimilation system (Bonavita and Torrisi, 2003) has been designed and implemented at the National Center for Aeronautic Meteorology and Climatology of the Italian Air Force (CNMCA) in order to improve its operational numerical weather prediction capabilities and provide more accurate guidance to operational forecasters. The system is based on an "observation space" version of the 3D-Var method for the objective analysis component (Cohn et al., 1998), and on the High Resolution Regional Model (HRM) of the Deutscher Wetterdienst (DWD) for the prognostic component (Majewski, 2001). Notable features of the system include a completely parallel (MPI+OMP) implementation of the solution of analysis equations by a preconditioned conjugate gradient descent method; functional representation of background error correlations in spherical geometry with thermal wind constraint between mass and wind field; derivation of the objective analysis parameters from a statistical analysis of the innovation increments.

The analysis and forecast fields derived from the assimilation system are objectively evaluated through comparisons with parallel runs based on the previous Optimum Interpolation based operational analysis and on the European Centre for Medium Range Weather Forecast (ECMWF) analyzed fields. Objective comparisons with RAOB and conventional surface observations are also presented in Bonavita and Torrisi, 2003. The main result of these studies is that, despite its relative simplicity, the new system is capable of adequately capturing the information content of the available observations, while the efficient parallel implementation of the objective analysis algorithm makes it suitable for operational use even in small operational environments.

Current Development Activities

Current activities focus on the continued development and extension of the data assimilation system:

1. Increase the forecast model horizontal resolution from the current 0.5° to 0.25° on the integration domain shown in fig.1. This is expected to improve the realism of the model forecasts especially in the lower troposphere, thus allowing for a larger number of surface and low level observations to be successfully ingested;

2. Observing system experiments (OSEs) to evaluate the impact of asynoptic observations on the analysis and forecast fields. Although it may be argued that the Euro-Atlantic integration domain is an area relatively well covered by the conventional observing network, encouraging results have been recorded so far from the inclusion of satellite-derived wind vectors. In fig.2 the impact of Quickscat derived winds on the Mean Sea Level Pressure forecast fields is shown. A small but persistent positive impact can be seen from the +18h forecast onwards. More impressive results are being obtained from the ingestion of METEOSAT Atmospheric Motion Vectors (AMV). Fig. 3 shows the importance of this type of observations in improving the wind field forecasts for almost all tropospheric levels, while the multivariate character of the objective analysis projects the geostrophic component of the information on the temperature field (fig. 4)

3. Another active field of activity is the implementation of interactive 1DVAR retrievals of temperature and humidity profiles from ATOVS radiances, for their subsequent ingestion in the objective analysis. This is considered an intermediate but necessary step towards the direct assimilation of ATOVS radiances. Work is now focusing on bias removal, cloud clearing algorithms and quality control of the observations.

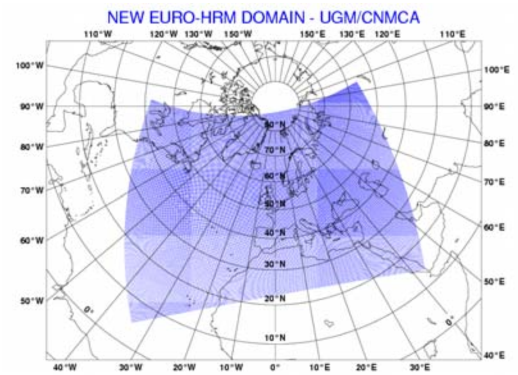

Figure 1. CNMCA Regional Model (EURO-HRM) domain of integration.

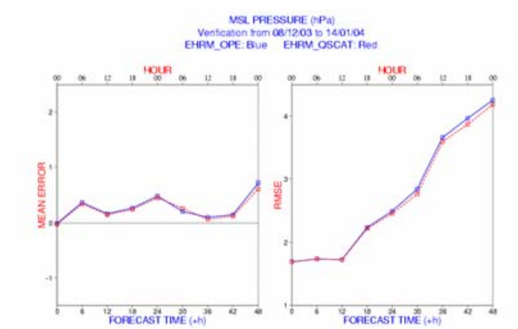

Figure 2. Mean and RMS error of EURO-HRM Mean Sea Level Pressure forecasts from CNMCA 3dVar analysis with (red) and without (blue) the ingestion of Quikscat winds verified against surface observations covering the entire integration domain.

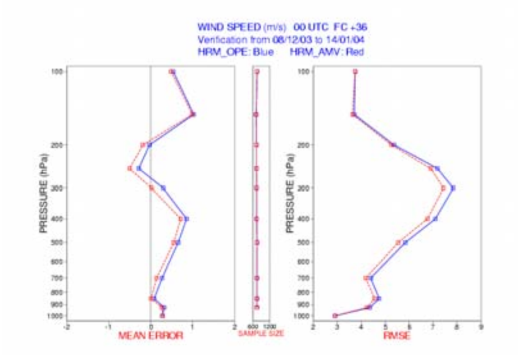

Figure 3. Mean and RMS error of EURO-HRM +36h wind speed forecasts from CNMCA 3dVar analysis with (red) and without (blue) the ingestion of AMV winds verified against RAOB observations covering the entire integration domain.

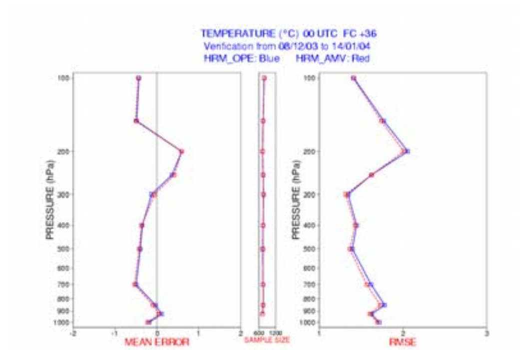

Figure 4. Mean and RMS error of EURO-HRM +36h Temperature forecasts from CNMCA 3dVar analysis with (red) and without (blue) the ingestion of AMV winds verified against RAOB observations covering the entire integration domain

REFERENCES

Bonavita, M. and Torrisi, L. (2003): " Impact Of a Variational Objective Analysis Scheme On a Regional Area Numerical Model: The Italian Air Force Weather Service Experience ", accepted for publication on *Journal of Meteor. And Atmos. Phys.*.

Cohn, S. E., Da Silva, A., Guo, J., Sienkiewicz, M. and D. Lamich (1998): "Assessing the Effects of Data Selection with the DAO Physical-Space Statistical Analysis System ". *Mon. Wea. Rev.*, Vol. **126**: 2913-26.

Majewski, D. (2001): "HRM User's Guide", available from the author (detlev.majewski@dwd.de)

Estimation of observation error statistics, using an optimality criterion

B.Chapnik*, G.Desroziers*, F.Rabier* and O.Talagrand**
* Météo France, CNRM **CNRS, LMD

Desroziers and Ivanov's method (2001)

Let B and R be the background and observation error covariance matrices specified in an operational data assimilation system and let $\mathrm{B_t}$ and $\mathrm{R_t}$ be the "true" matrices. Assuming that one can write

$$\mathrm{B_t}= s_b\, \mathrm{B},\ \mathrm{R_t}= s_o\, \mathrm{R},\ \text{or}\ \mathrm{R_{tk}}= s_{ok}\, \mathrm{R_k},\ \mathrm{B_{tl}}= s_{bl}\, \mathrm{B_l},$$

where the k and l subscript refer to statistically independent subparts of the observations and of the control vector , the aim of this work is to evaluate the tuning coefficients: s_o and s_b (s_{ok} and s_{bl})
Desroziers and Ivanov (2001) proposed to use an optimality criterion found by Talagrand (1999).
The tuning coefficients are those for which this criterion if fulfilled.
If $\boldsymbol{x_a}$ is the minimizer of J_t then, following Talagrand (1999), the expectations of the subparts of the cost function at the minimum are:

$$\mathbf{E(2J_{ok}(\boldsymbol{x_a})/s_{ok})=Tr\ [\pi_k(I_p - HK)\pi_k^T]}$$
$$\mathbf{E(2J_{bl}(\boldsymbol{x_a})/s_{bl})=Tr\ (\pi_l KH\pi_l^T)}.$$

Where **E** is the expectation operator, **K** is the gain matrix, **H** is the observation operator, and $\boldsymbol{\pi_k}$ and $\boldsymbol{\pi_l}$ are the projections onto the k^{th} type of observations and to the l^{th} independent subpart of the control vector. The tuning coefficients are computed as the limit of a fixed point algorithm, going from step *i* to step *i+1* using the following relations:

$$s^{(i+1)}_{ok}= 2J_{ok}(\boldsymbol{x_a}(\mathbf{s}^{(i)}))/\ \mathrm{Tr}\ [\pi_k(\mathbf{I}_p - \mathbf{HK}^{(i)})\pi_k^T],\ \forall k$$
$$s^{(i+1)}_{bl}= 2J_{bl}(\boldsymbol{x_a}(\mathbf{s}^{(i)}))/\ \mathrm{Tr}\ (\pi_l\mathbf{K}^{(i)}\mathbf{H}\pi_l^T),\ \forall l.$$

Chapnik *et al*. (2003) have shown that the method is equivalent to a Maximum likelihood tuning of the variances. (Dee and da Silva 1998); therefore, the quality of the estimates depends on the number of observations and on the quality of the *a priori* modelization of covariances. The computed values are temporally stable (up to four years); on the contrary they react quickly and increase when the quality of observations is degraded: they behave like variances are supposed to.
Moreover, as already stated by Desroziers and Ivanov, the first fixed-point iteration yields a good approximation of the final result making the following implementation of the algorithm feasible: only one fixed point iteration is used ands several situations were "concatenated" to increase the accuracy of the estimate. The estimation of the kth observational tuning coefficient becomes:

$$s_{ok}=\left(\boldsymbol{\Sigma_i}\ \mathbf{J_{ok}^i}(\boldsymbol{x_a})\right)\ /\ \left(\boldsymbol{\Sigma_i}\ \mathrm{Tr}\ [\pi_k(\mathbf{I}_{pi} - \mathbf{H^iK^i})\pi_k^T]\ \right),$$

where i refers to the i^{th} situation. The different situations used in the computation are separated by at least 5 days in order to prevent time correlation.

Results with simulated and real satellite radiances

Figure 1 shows the ability of the method to retrieve optimal variances in a simulated case. In this case the true standard deviations are the operational values and the mis-specified standard deviations are equal to the square root of the operational values; six dates, separated by more than five days, between 03/15/2003 and 05/19/2003 were used. Another computation was carried out with more thinning of the data in order to check the impact of a smaller number of observations. The standard deviations were computed for each of the three satellites NOAA15, NOAA16 and NOAA17, for sea pixel observations. In all cases the computed deviations are fairly close to the expected ones.
The result of the same computations, carried out with actual data, is shown in Fig. 2. Roughly, all the standard deviations are over estimated by a factor of 2. Satellite NOAA16 instrument seems to have a larger standard deviation for channel 8 than the other satellites. The standard deviations computed with a twice larger thinning interval are almost always larger than those computed with the operational thinning, which does not appear in the simulated case, possibly due to spatial or inter-channel correlation.

Similar computations were also carried out with well-documented data (TEMP profiles). The tuned variances remained close to the prescribed ones (not shown).

Conclusions and future directions.

The first iteration of Desroziers and Ivanov's algorithm, cumulating the observations over several dates, has been shown to be able to produce reliable estimates in a simulated case, its application to ATOVS radiances show several possibly useful and unexpected features but the role of possible correlations has to be clarified. Its application to well-documented data is encouraging. Future work will extend to the tuning of all observation types and a level by level tuning of B in order to evaluate the impact of this tuning on the analysis and on the forecasts.

References

B. Chapnik, G. Desroziers, F.Rabier and O.Talagrand. 2003,
Properties and first applications of an error statistic tuning method in variationnal assimilation. Submitted to Q.J.R.M.S

G. Desroziers and S. Ivanov. 2001,
Diagnosis and adaptive tuning of information error parameters in a variational assimilation.
Quart. J. Roy. Meteor. Soc., 127, 1433--1452

D. Dee and A. da Silva. 1998,
Maximumlikelihood estimation of forecast and observation error covariance parameters. part I: Methodology.
Mon. Wea. Rev., 124:1822--1834.

O. Talagrand. 1999;
A posteriori verification of analysis and assimilation algorithms.
In Proceedings of the ECMWF Workshop on Diagnosis of Data Assimilation Systems, 24 November pages 17--28, Reading

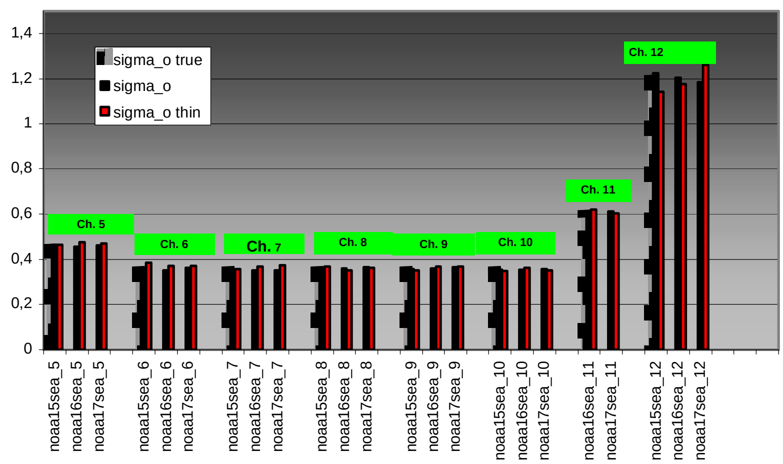

Figure. 1: Standard deviations of AMSU A channels obtained by the method in a simulated case. The black bars are computed with the operational thinning between obs. and the red bars with a twice larger thinning interval. A different deviation is computed for each satellite , a difference is also made between sea and land observations. The grey bars with dots show the simulated « true » standard deviations.

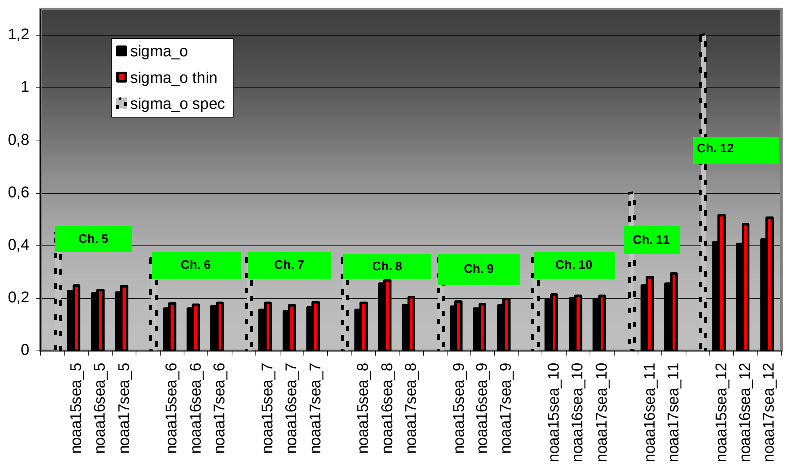

Figure 2: Standard deviations of AMSU A channels obtained by the method in a true case. Plotting conventions are the same as in Fig. 1 but this time the grey bars with black dots are the prescribed standard deviations

Assimilation of MODIS wind data in the global NWP System of the German Weather Service

Alexander Cress, Deutscher Wetterdienst, P.O. BOX 106465, 63004 Offenbach am Main Germany
email: Alexander.Cress@dwd.de

Global measurements of wind field is essential to improve our knowledge of atmospheric dynamics, including atmospheric transport processes of energy, water and airbourne particles. Unfortunately, coverage of wind observations is rather poor over the oceans, and the polar regions. Only a few regular wind measurements are made along the coastal areas of the Arctic, Antarctica and the interior of Canada, Alaska, Russia and Northern Europe, but there is little or no coverage of the interior of Antarctica, Greenland or the Artic Ocean. Poor knowledge of the polar wind field is a major cause of larger than normal analysis and forecast errors in these regions, leading to occasional forecast 'busts' in areas like Europe, influenced by synoptic disturbances originating in polar regions.

Recently a new satellite-derived wind product has become available, which provides polar wind fields. The winds are derived by tracking features in the IR window band at 11μm and in the water vapour (WV) band at 6.7μm from the Moderate Resolution Imaging Spectrodiameter (MODIS) instrument on board the polar-orbiting satellites Terra and Aqua. Wind vector heights are assigned by using either the IR window, CO_2 slicing or the H_2O intercept method (Key et al., 2002). Results of the NOGAPS model are used as a first guess. MODIS data are available in areas north of 60^oN and south of 60^oS.

Using the global assimilation and forecasting system of the German Weather Service (DWD), two impact experiments - one summer (June 2003) and one autuum case (October 2003) - were conducted to estimate the potential benefit of the MODIS wind observations. In contrast to the operational use of AMW winds from geostationary satellites (only over oceans), the experiments used the MODIS wind observations over land and ocean. Due to problems with height assignment and topography (Key, 2002), the MODIS WV winds were used above 400 hPa only and the MODIS IR winds over Antarctica above 550 hPa only. The winds were thinned to 70 km resolution and quality controlled in the same way as the AMV winds of the geostationary satellites. As a control run, the operational assimilation and forecast system at DWD were used, with a variety of conventional (radiosondes, aircraft, synops, buoys) and satellite (SATOB, SATEM) data.

Various aspects of the quality of MODIS data were investigated, such as frequency distributions or time series of differences between observations and first guess before and after the quality control. A good correspondence was found between the MODIS statistics and similar statistics for AMV winds from geostationary satellites (Fig. 1). Obviously, there is a positive bias between observations and model (model too slow), which is stronger in the Southern Hemisphere than in the Northern Hemisphere. Comparing the two satellites Terra and Aqua, a higher OBS-FG bias could be found for Aqua, especially over Antarctica (not shown). The MODIS winds have a large impact on the DWD polar analysis by introducing analysis increments in data void areas. The overall impact on forecast quality is small but positve for Europe and the Northern Hemisphere and neutral for the Southern Hemisphere for the summer case, although periods can be detected, were using the MODIS wind data leads to a substantial improvement of the forecast quality (Fig. 2; end of the period). The autumm case shows the opposite behaviour; a neutral impact for Europe and the Northern Hemisphere, and a small positive impact for the Southern Hemisphere (not shown). Obviously, the impact on forecast quality depends strongly on season and occasions in which the interaction between polar and midlatitude flow patterns is particularly intense. The relatively minor impact of the MODIS data on the Southern Hemisphere could be connected to height assignment problems over high topography or conditions such as low-level thin stratus, which make it difficult to indentify trackable features over the Antarctic continent.

References

Key, J.R. Santek, D. C.S. Velden, Bormann, N. Thepaut, J.-N. Riishojgaard, L.P. Zhu, Y. Menzel, W.P., 2002: *Cloud-drift and water vapor winds in the polar regions from MODIS,* IEEE Transactions on Geoscience and Remote Sensing, 41, 482-492.

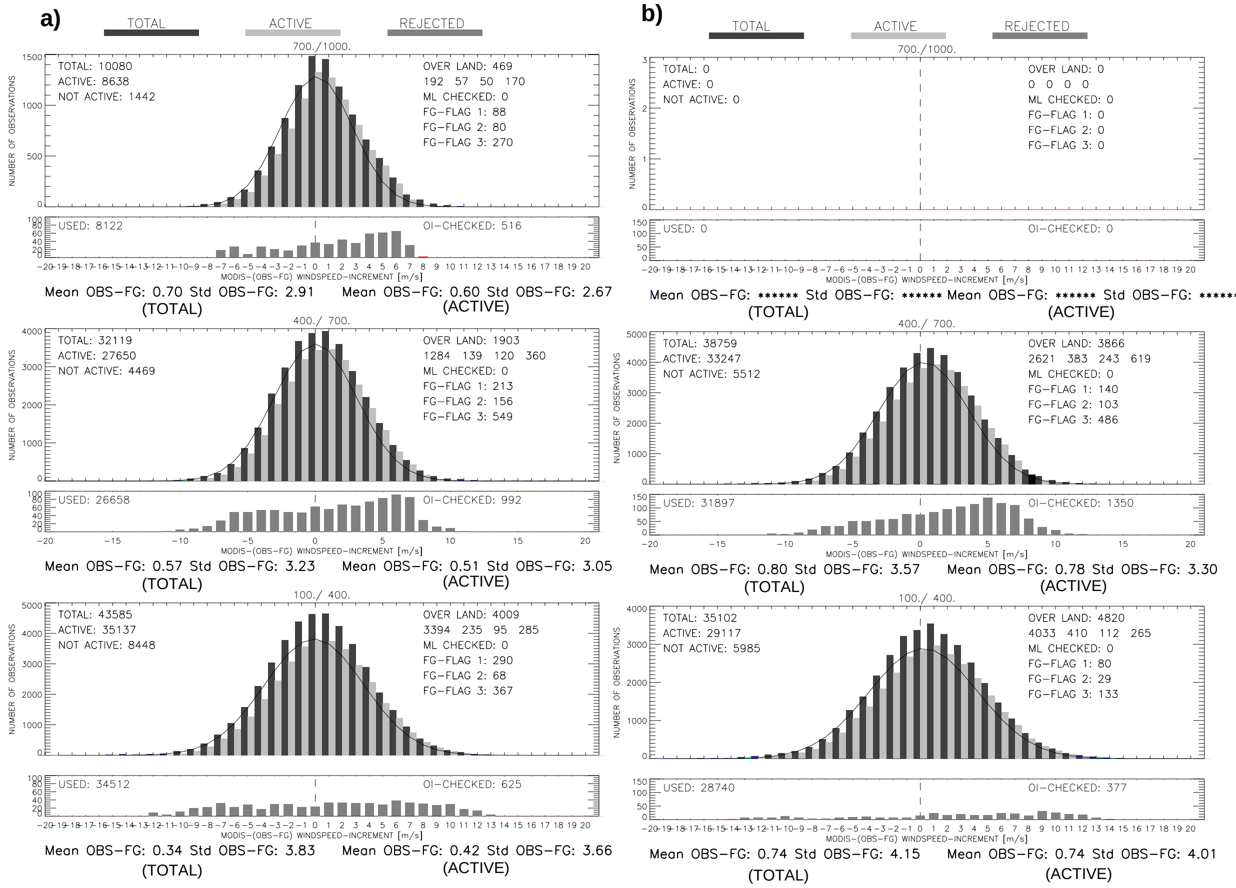

Figure 1: Frequency distribution of the difference between Modis windspeed (Terra and Aqua) and first guess, including quality control statistics for the summer case (June 12 to July 9, 2003) for all (Total, dark columns), active (after the quality control; light shaded columns) and used (after quality control and OI check, shaded columns in bottom picture) wind data, including the mean and standard deviation for all and active data, separated for the Northern (a) and Southern Hemisphere (b).

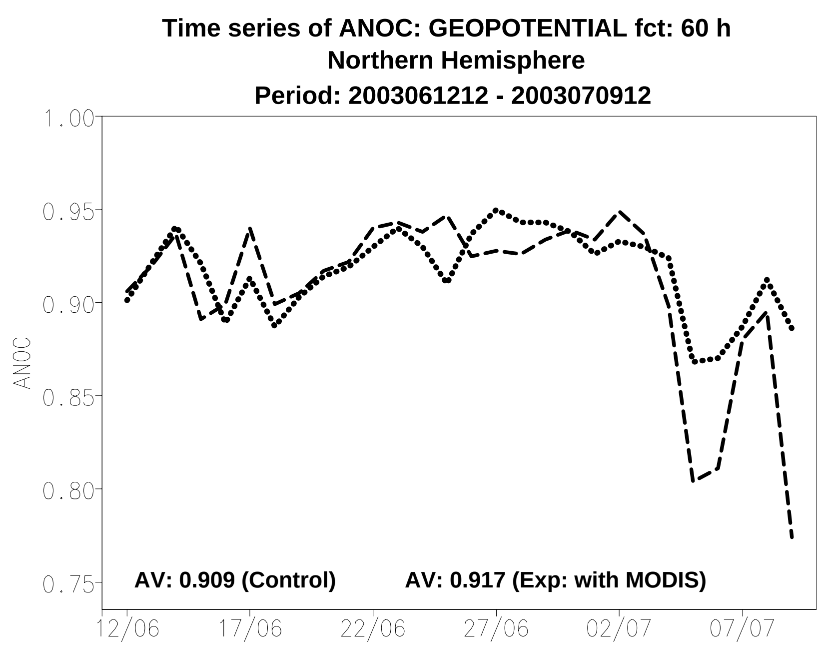

Figure 2: Time series of anomaly correlation coefficients of the 500 hPa geopotential height for the Northern Hemisphere at forecast time of 60h for control (dashed) and experiment (dotted) forecasts, including the MODIS wind data, from June 12 to July 9, 2003 12 UTC.

Use of dropsonde data in the global data assimilation of the German Weather Service

Alexander Cress, Deutscher Wetterdienst, P.O. BOX 106465
63004 Offenbach am Main
Germany
email: Alexander.Cress@dwd.de

Numerical weather prediction systems require exact three-dimensional global observations of wind, temperature, humidity etc. as initial conditions to achieve a skillful weather forecast. The lack of an adequate observation network over the oceans can result in fast-growing analysis errors leading to poor forecasts of oceanic cyclones such as extra-tropical low pressure systems or severe tropical storms (hurricanes, typhoons). Observation targeting can be a successful concept to provide measurements in data-sparse oceanic areas in cases of tropical storms or in sensitive regions where errors in the initial state are fast-growing. The major observational tool for targeting is a dropsonde, released from aircraft over sensitive areas to measure wind, temperature and humidity profiles.

In preparation for the Atlantic-Thorpex Observing System Test (TOST) experiment (October - December 2003; Truscott, 2003) the German Weather Service (DWD) expended some effort to decode and use dropsonde data in its global assimilation and forecast system. As a first test case, seventy-one dropsonde profiles taken by NASA and NOAA hurricane flight missions on 18 Sept. 2003 over hurricane Isabel shortly before landfall became available over GTS (Fig. 1).

The operational global data assimilation and forecasting system of the DWD was used to assimilate dropsonde wind, temperature and humidity profiles; here, the observation error assigned to the data was unchanged with respect to the radiosonde observations. In order to estimate the potential benefit of dropsonde data, the analysis and forecast was compared to a control run using the operational assimilation and forecast system at DWD, with a variety of conventional (radiosonde, aircraft, synops, buoys) and satellite (SATOB, SATEM) data but without any dropsonde measurements.

The operational analysis without dropsonde data considerably overestimated the surface pressure in the center of hurricane Isabel, and therefore, underestimates the maximum wind speeds (Fig. 2a). Using the temperature, wind and humidity profiles from the dropsondes in the assimilation reduces the surface pressure in the center of hurricane Isabel by more than 20 hPa (Fig. 2b), leading to a more realistic analysed maximum wind speed and a better track and intensity forecast of the tropical storm system after landfall (not shown).

References

Truscott, B., 2003: *Atlantic-Thorpex Observing System Test Project Plan,* EUCOS/SP/105 version 4

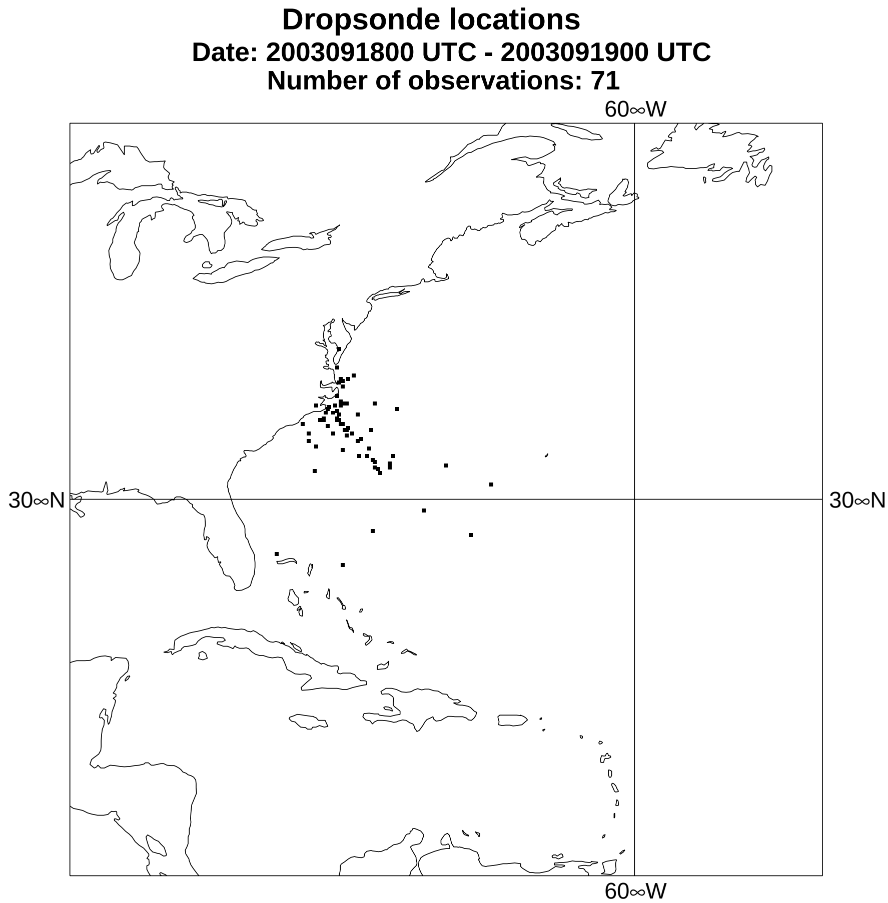

Figure 1: Location of Dropsondes providing data to DWD from 20030918 to 20030919 (black dots).

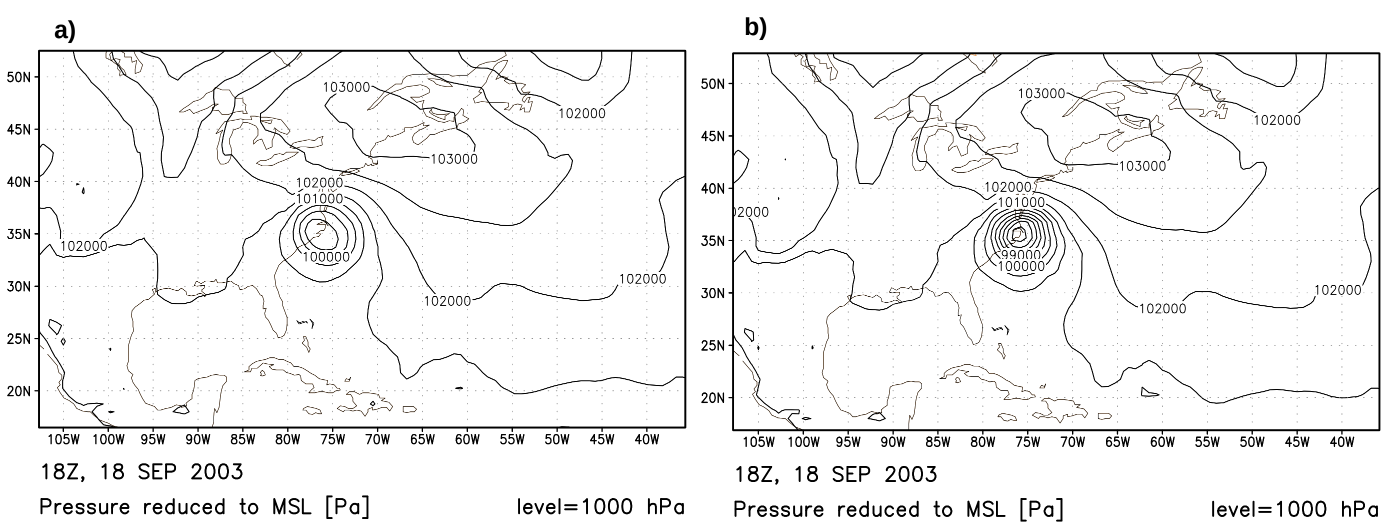

Figure 2: Analyses of sea surface pressure [Pa] at 18.09.2003 18 UTC for (a) the Routine (center pressure < 995 hPa) and (b) an experiment using the dropsonde data (center pressure < 975 hPa) since 20030918 00 UTC.

Assimilation of ozone retrievals from the MIPAS instrument on board ENVISAT at ECMWF.

Antje Dethof

Ozone retrievals from satellites have been assimilated in the operational ECMWF system since April 2002. At the beginning, total column ozone retrievals from GOME (Global Ozone Monitoring Experiment) on ERS-2 provided by KNMI's Fast Delivery Service, and ozone layers from the SBUV/2 (Solar Backscatter Ultra Violet) instrument on NOAA-16 were used in the operational assimilation system. The SBUV/2 data are given as 12 ozone layers and are combined at ECMWF into 6 layers (0.1-1 hPa, 1-2 hPa, 2-4 hPa, 4-8 hPa, 8-16 hPa, 16 hPa-surface) to reduce vertical observation error correlations. This means that the ozone data assimilated at ECMWF were in effect total column data, as the lowest SBUV layer spans from 16 hPa to the surface. The assimilation of ozone retrievals in such broad layers can lead to problems with the vertical structure of the analysed ozone field if there is a systematic bias between the model and the data (Dethof and Hólm 2003). In these situations there is not enough vertical resolution in the observations to assign the analysis correction to the right levels. Instead, the information about how to distribute the analysis correction increment in the vertical has to come from the background error covariances. The background errors, however, only describe random errors and not systematic ones, and when systematic biases are interpreted as random errors by the analysis, this can lead to corrections being applied to the wrong level.

It was hoped that the ozone analysis could be improved by assimilating ozone data with a higher vertical resolution than the data used initially at ECMWF. Such ozone data became available after the launch of the ENVISAT satellite on 1 March 2002. One of the instruments on board ENVISAT is MIPAS (Michelson Interferometer for Passive Atmospheric Sounding), a limb-viewing high-resolution Fourier-transform spectrometer, that measures atmospheric emissions in the mid-infrared part of the spectrum between 4.15 and 14.6 microns. MIPAS provides global coverage, including coverage of the polar regions, independent of illumination conditions, and allows the retrieval of ozone profiles from the model top at 0.1 hPa down to about 200 hPa with a vertical resolution of 3-5 km. This means MIPAS profiles have a better vertical resolution than the ozone data originally used at ECMWF.

The assimilation of MIPAS ozone retrievals was tested at ECMWF. It leads to a pronounced improvement of the ECMWF ozone analysis in the extratropics, both in the total column ozone field and in the vertical ozone distribution, while the impact on the forecast scores is neutral. Assimilation experiments show that in February 2003 the impact of assimilating MIPAS ozone profiles is strongest at high latitudes of the northern hemisphere (NH), where total ozone values are reduced, giving a better agreement of the ECMWF ozone field with independent TOMS data, and also a better agreement of analysis ozone profiles with ozone sondes. In August and September 2003 the impact is strongest in the southern hemisphere (SH), where the representation of the Antarctic ozone hole in the analysis is improved when MIPAS ozone data are assimilated.

Figure 1 compares ozone profiles from an experiment with (red curve) and without (green curve) the assimilation of MIPAS ozone profiles with independent ozone sonde

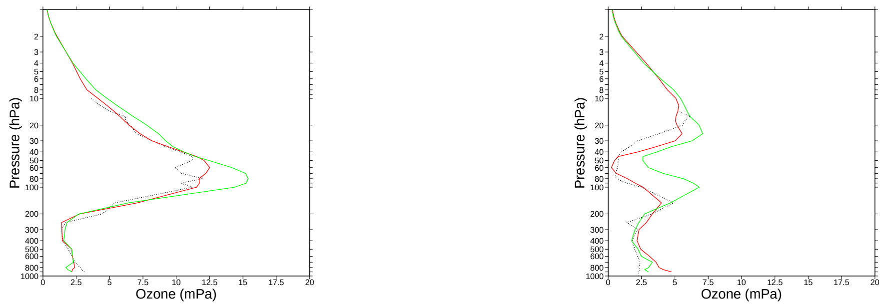

Figure 1: Ozone profiles in mPa from sondes (black), an experiment with the assimilation of MIPAS ozone profiles (red), and an experiment without the assimilation of MIPAS ozone profiles (green) from the Antarctic Neumayer station (71°S, 8°W) on 26 August (left) and 1 October 2003 (right).

observations from the Antarctic Neumayer station on 26 August and 1 October 2003. The ECMWF model has a positive ozone bias over the South Pole during southern winter and spring. During the ozone hole season, the chemistry parameterization is not able to reduce ozone values to the very low values seen in observations. At this time of year, the assimilation of MIPAS ozone data has a large impact on the shape of the analysis profile at the Antarctic Neumayer station, and the analysed ozone field is much improved if MIPAS ozone profiles are assimilated. In August the ozone layer over the South Pole has started to thin, but is not completely destroyed yet. The ECMWF analysis without the assimilation of MIPAS ozone profiles overestimates the ozone values at and above the ozone maximum. When MIPAS data are assimilated ozone values are reduced and the agreement with the sonde is good. At the beginning of October the ozone hole is fully developed, and ozone is almost completely deleted between 100-40 hPa. When MIPAS ozone data are assimilated the analysis profile agrees well with the sonde, while the analysis without MIPAS data does not reproduce the very low values seen in the observations. The resulting total column ozone field also agrees better with independent TOMS observations over the South Pole if MIPAS ozone profiles are assimilated (not shown).

The main reason the assimilation of MIPAS ozone profiles has a positive impact on the vertical structure of the analysed ozone field over most of the globe is the higher vertical resolution of the MIPAS profiles, compared to the ozone data previously assimilated at ECMWF. Information about the vertical structure of the analysis correction now comes from the data, and does not have to be inferred from the background error statistics. Furthermore, it is beneficial that MIPAS provides day and night time measurements, including coverage of the poles during the polar night.

Owing to the positive impact on the ozone analysis, the assimilation of MIPAS ozone profiles was included in the operational ECMWF system in October 2003.

References

Dethof, A., and Hólm, E.V. (2003). Ozone assimilation at ECMWF. *Quart. J. Roy. Meteor. Soc.*, 128. submitted.

Revision of the Background Error Covariance in the Global 3D-Var Data Assimilation System

Tadashi Fujita
Numerical Prediction Division, Japan Meteorological Agency,
1-3-4 Otemachi, Chiyoda-ku, Tokyo 100-8122, Japan
e-mail: t-fujita@met.kishou.go.jp

A 3D-Var data assimilation system was implemented in the operational global analysis at JMA in September 2001 (Takeuchi and Tsuyuki, 2002). Although the 3D-Var system has brought much improvement on the operational numerical weather prediction at JMA, there have been a problem that the background error correlation was too strong at large scales, so that each observational datum affected undesirably wide range of the field in data assimilation. It was recently found that the cause of the problem was an artificial smoothing operated on the vorticity background error covariance. The smoothing was originally introduced in order to suppress the horizontal correlation of the control variables at large distances. The smoothing, however, was found to have a side effect of excessive correlation in the vorticity-balanced part of the increment at low frequencies.

Figure 1 displays the increment in surface pressure dP_S when a single P_S observational datum is assimilated. With the artificial smoothing operated on the background error covariance, the increment is spread over wide range. Without the smoothing, it is reasonably localized around the datum point. Figure 2 displays the power spectrum of the increment of modified balanced mass variable df_B, which accounts for much of the increment dP_S, and which directly reflects the properties of the background error covariance of the vorticity field at low frequencies. It can be seen from the figure that the amplitudes of the increment df_B at low frequencies are unnatural when the smoothing is operated.

Figure 3 displays the time-series of the analyzed temperature at 300 hPa, averaged over the antarctic region. The time-series are obtained by cycled analyses performed under several different conditions. The result obtained from the global analysis by UK Met Office (UKMO) is also shown for reference. The temperature suddenly rises at 12 UTC September 25, 2001, when the assimilation method changed from OI to 3D-Var with the artificial smoothing on the background error covariance ("OI $\rightarrow$ 3DVAR" line). In order to moderate the sudden change of the temperature, a modification was applied in the operational process at JMA on the regression coefficient between the background error of modified balanced mass variable and that of unbalanced temperature ("RTN" line). In this case, the temperature is almost steady but systematically higher than that obtained by OI. Drastic changes in the temperature can be averted without applying any modification on the regression coefficient, if 3D-Var was performed without the artificial smoothing on the background error covariance ("without smoothing" line).

Following the investigation described above, the artificial smoothing on the background error covariance and the modification on the regression coefficient were stopped in the operational 3D-Var system at JMA in May 2003.

References

Takeuchi, Y. and Tsuyuki, T., 2002: The operational 3D-Var assimilation system of JMA for the Global Spectrum Model and the Typhoon Model. In: *Research Activities in Atmospheric and Oceanic Modelling*, H. Ritchie (Ed.), Volume No. 32, WMO/TD-No. 1105, pp. 1.59 – 1.60. WMO.

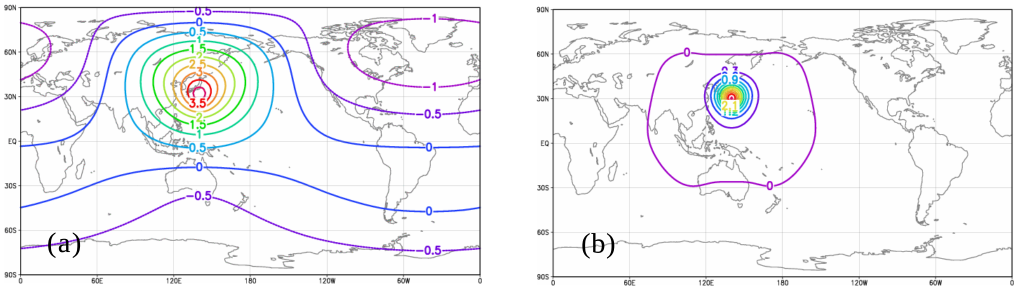

Fig. 1 Increment in P_S when a single P_S observational datum is assimilated. The datum is put at the point (30N,140E). (a): with smoothing, (b): without smoothing.

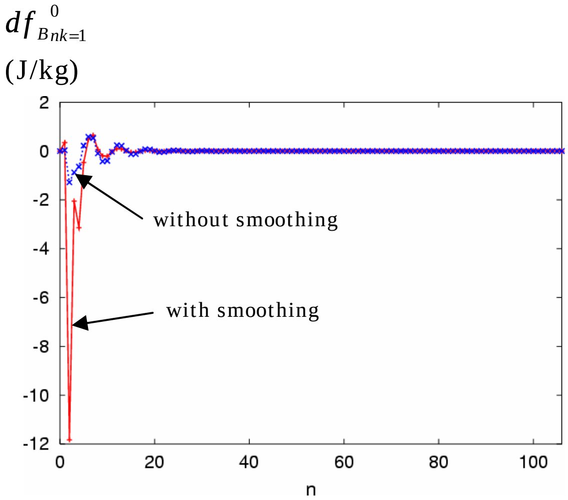

Fig. 2 Power spectrum of df_B. The result is displayed for the lowest model level, and for zonal wavenumber $m = 0$.

(n : total wave number)

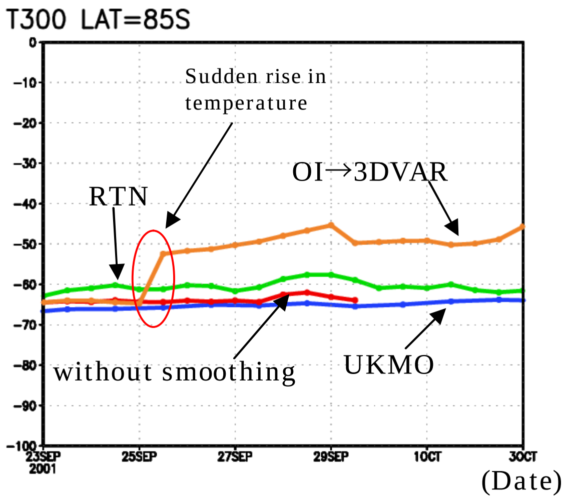

Fig. 3 Time-series of analyzed antarctic temperature (in centigrade) at 300 hPa, averaged over the circle of latitude 85S.

i) OI→3DVAR: Analysis method changed from OI to 3D-Var at 12UTC Sep. 25, 2001. The 3D-Var is performed with the artificial smoothing on the background error covariance.

ii) RTN: 3D-Var implemented in the operation at JMA. With the smoothing on the background error covariance. Modification on the regression coefficient is applied.

iii) UKMO: Global analysis by UKMO.

iv) without smoothing: 3D-Var without the smoothing on the background error covariance. The modification on the regression coefficient is not applied.

Improvements of ATOVS radiance-bias correction scheme at JMA

Masahiro Kazumori, Hiromi Owada, Kozo Okamoto
Numerical Prediction Division, Japan Meteorological Agency
1-3-4 Otemachi, Chiyoda-ku, Tokyo 100-8122,JANAN

email: kazumori@met.kishou.go.jp,
howada@naps.kishou.go.jp ,okamoto@npd.kishou.go.jp

1. Introduction

JMA has started operational use of ATOVS radiances in the global data assimilation on 28 May 2003. ATOVS radiances replaced retrievals of ATOVS from NOAA/NESDIS and that of GMS-5. The effect of direct assimilation of ATOVS radiances was dramatic. The temperature profiles in the upper stratosphere and global humidity field in the troposphere were improved compared with retrieval assimilation. As for forecast skills, positive impacts were found for the geopotential height at 500 hPa especially in the Southern Hemisphere and in the tropical region. The improvement of forecast skill in short-term forecasts was remarkable, and better results on the typhoon track prediction were also found. JMA has achieved considerable progress in ATOVS data assimilation, but some un-preferable features are still seen: anomalous profile of temperature at some levels in the stratosphere. To solve this problem, we continue to carry out some experiments with an improved bias correction scheme of ATOVS brightness temperature.

2. Upgrade of radiance-bias correction

JMA radiance-bias correction scheme is based on radiosonde observation (Kazumori et al. 2003). Due to lack of radiosonde data (temperature in stratosphere and moisture in troposphere), six-hour forecasts were used to make up the profile to calculate radiance in a radiative transfer model (RTTOV-6, Saunders 1998). In the current ATOVS radiance assimilation system at JMA, radiance-bias correction is not employed for AMSU-A upper stratosphere channels 12, 13, 14 and AMSU-B moisture channels 3, 4, 5, and HIRS/3 moisture channels 11, 12, because there are some biases in stratospheric temperatures and tropospheric moisture in the JMA global model.

It is well known that raw radiances from satellite have instrumental biases and there are some biases in the radiative transfer model. Through the operational use of ATOVS radiances at JMA, anomalous changes of temperature at some levels in the stratosphere have been detected. To remove stratospheric temperature biases in analysis field, an improved radiance bias correction scheme was applied to the upper stratosphere channels and the moisture channels. To make the scheme reliable, a period of collocation of radiosonde and satellite was extended from one year to two years. Besides a scan bias correction was implemented in moisture channels of AMSU-B.

3. Results

To confirm the effect of upgrade of the bias-correction scheme, cycle experiments were carried out for December 2002. Low-resolution system of T106L40 3D-Var and the JMA Global Spectral Model was used. The experimental configuration is as follows,

Test: Improved radiance-bias correction scheme.

Cntl: Operational radiance-bias correction scheme.

Figure 1 shows the global mean temperature profile of analysis field at 00UTC 31 December 2002. Cooling bias in stratosphere from 10hPa to 2hPa was reduced and temperature profile was improved particularly in the upper stratosphere compared with Cntl run. Figure 2 shows time sequences of difference of the background temperature and radiosonde temperature observations in the Northern Hemisphere for December 2002. Clear improvements of BIAS and RMSE were found at stratosphere temperature from 30 hPa to 10 hPa. As for forecast skill, positive impact was found in the 500 hPa geopetential height.

Furthermore, we are going to carry out experiments for two seasons using JMA full resolution data assimilation system to confirm the forecast impacts. This new radiance-bias correction will be implemented in the JMA operational global data assimilation system in 2004.

References

Kazumori, M., K. Okamoto, and H. Owada, 2003: Operational use of ATOVS radiances in global data assimilation at the JMA, *Tech. Proc. of 13th International TOVS Study Conference, Quebec, Canada 29 Oct. -4 Nov. 2003.* (Submitted)

RTTOV-6 SCIENCE AND VALIDATION REPORT 2000. Available from the NWP SAF web site.[1]

Saunders, R., M. Matricardi and P. Brunel, 1998: An improved fast radiative transfer model for assimilation of satellite radiance observations. *Q. J. R. Meteorol. Soc.*, 125, 1407-1425.

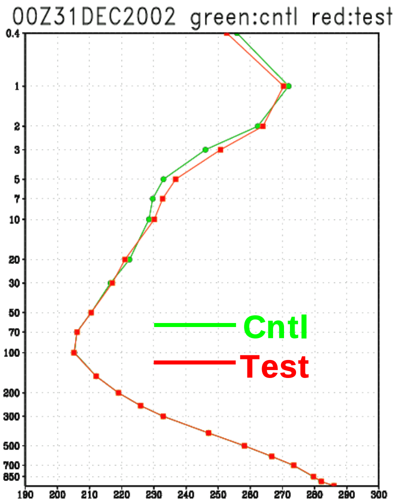

Fig. 1: Global mean temperature profile of analysis field at 00UTC 31 December 2002. Red line is temperature profile of Test run, and green line is that of Cntl run.

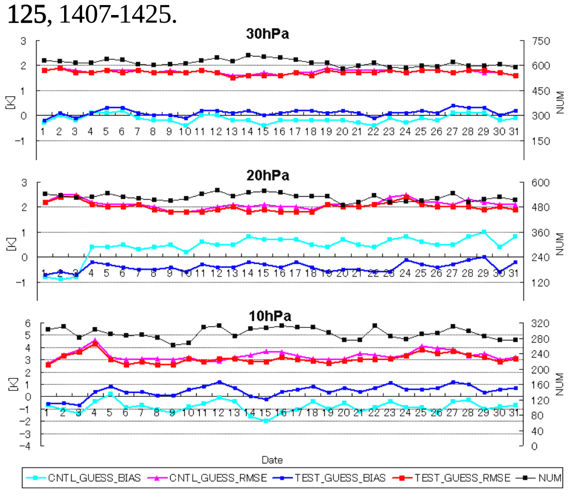

Fig. 2: Time sequence of difference between the background temperature and radiosonde observations in the Northern Hemisphere for December 2002. Upper panel is for 30 hPa, middle for 20 hPa, and lower for 10 hPa. (Test: Red line is RMSE and blue line is BIAS, Cntl:Light red line is RMSE and light blue is BIAS. Black line is number of sampled data for each experiment.)

[1] < http://www.met-office.gov.uk/research/interproj/nwpsaf/rtm/d81svr.pdf >

Adaptive algorithm of the suboptimal Kalman filter

Dr. Ekaterina G. Klimova
Institute of Computational Technologies,
Siberian Branch, Russian Academy of Sciences,
Ac. Lavrentjev Avenue, 6
Novosibirsk 630090 Russia
klimova@ict.nsc.ru

The most fundamental difficulties of the implementation of the Kalman filter theory to the meteorological data assimilation are that it is too computationally expensive and requires too much information [1]. One of the ways to solve this problem is to apply the simplified models in a Kalman filter for calculation of the forecast error covariances (suboptimal Kalman filter).

In the Kalman filter algorithm the forecast error covariance matrix P_k^f is calculated under the formula: $P_k^f = A_{k-1}P_{k-1}^a A_{k-1} + Q_{k-1},$ where A_{k-1} - describes the operator of forecast model, Q_{k-1} is the model error covariance matrix, P_{k-1}^a - the analysis error covariance matrix. In the suboptimal Kalman filter algorithm the on a step of calculation of a matrix P_k^f instead of the operator A_{k-1} the operator of the simplified model $\widetilde{A}_{k-1}$ (smaller dimension) is used. The variants of the simplified models for calculation of a matrix P_k^f are considered in works [2-5].

It is well known, that if Q_{k-1} is not sufficiently well known or if $Q_{k-1} = 0$, the Kalman filter may diverge [1]. In case the covariance matrix of model noise is set zero, there is a fast decrease of theoretical error of the Kalman filter algorithm and, as a consequence, the observations enter on an analysis step with the lesser factors. This effect is named “divergence of the Kalman filter algorithm”. In the given work the adaptive Kalman filter algorithm of estimation of Q_{k-1} is considered. The algorithm allows correct the forecast error covariance matrix P_k^f, calculated with the help of the simplified operator $\widetilde{A}_{k-1}$, also. The algorithm is based on use of vectors of “residuals” (difference between observations and forecast). The forecast of P_k^f with the use of $\widetilde{A}_{k-1}$ we shall consider as the first guess of P_k^f. $\widetilde{A}_{k-1}$ can differ from operator of initial model, as in suboptimal algorithm of the Kalman filter. In adaptive algorithm the diagonal elements of P_k^f are calculated by the method of successive correction. In that method we use the residuals for obtaining the “observed” values of diagonal elements of P_k^f. A full matrix P_k^f we shall restore, considering, that correlations are calculated precisely.

On the fig.1 and fig.2 the dependence of weight coefficients in procedure of the analysis from the space is given. The weights were calculated for the one central point of the region for 0 hour (fig.1) and 12 hour (fig.2). On that figures through w_1 are designated weights calculated on a matrix P_k^f, obtained with the help of adaptive algorithm, w_2 - weights calculated on a matrix

P_k^f , obtained under condition $Q_{k-1} = 0$. So, when we suppose $Q_{k-1} = 0$, the weights become unreal small (Kalman filter diverge), the adaptive algorithm help to avoid the "divergence".

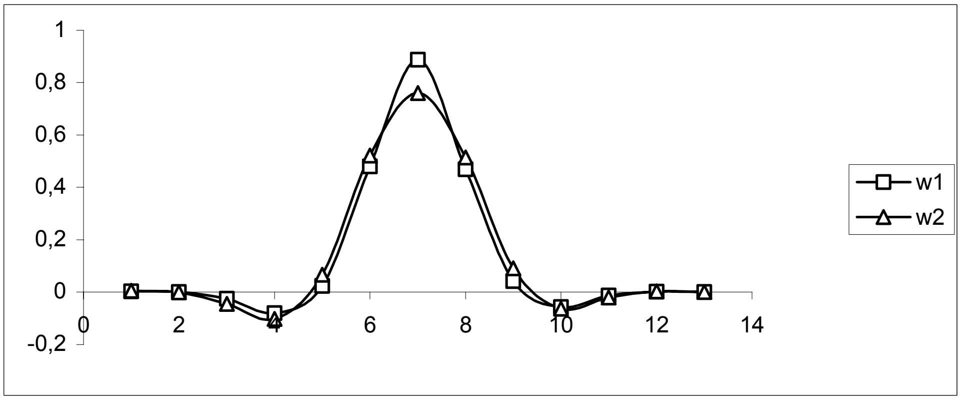

Fig.1

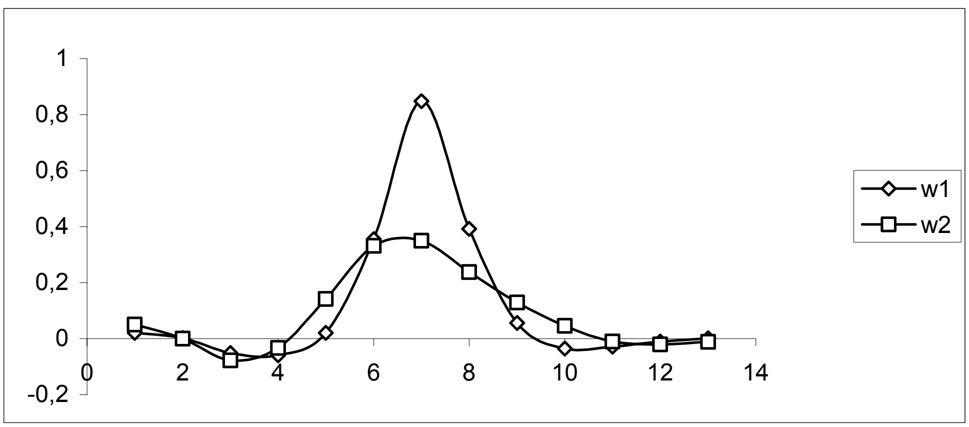

Fig.2

References

1. Jazwinski A.H. Stochastic processes and filtering theory. -Academic Press, New York, 1970.
2. E.G.Klimova. Simplified models for calculation of covariance matrices in the Kalman filter algorithm. - Meteorologiya i Hydrologiya, 2000, N 6. (Translated on English: Russian Meteorology and Hydrology).
3. E.G.Klimova. A model to calculate the covariances of homogeneous isotropic stochastic fields of forecast errors. - Meteorologiya i Hydrologiya, 2001, N 10.
4. E.G.Klimova. Model for calculation the forecast error covariances in the Kalman filter algorithm based on the full quations. - Meteorologiya i Hydrologiya, 2001, N 11.
5. E.G.Klimova. Numerical experiments on meteorological data assimilation with the help of the suboptimal Kalman filter. - Meteorologiya i Hydrologiya, 2003, N 10

Four-dimensional Variational Data Assimilation of TRMM Data in Tropical Cyclone Prediction

LEIMING MA*, YIHONG DUAN, XUDONG LIANG, DONGLIANG WANG
Shanghai Typhoon Institute, China Meteorological Administration, Shanghai, China
*Email: malm@mail.typhoon.gov.cn

1. Introduction

Many studies have indicated that inclusion of rainfall data into numerical models can improve the accuracy of numerical weather prediction (e.g. Krishnamurti et al. 1993). Recently, Pu et al. (2002) assimilated the Tropical Rainfall Measuring Mission (TRMM)/TRMM Microwave Imager-derived surface rainfall rate (SRR) into the Goddard Earth Observing System with the one-dimensional + four-dimensional data assimilation technique (Hou et al. 2000) in the numerical simulation of a mature tropical cyclone. This study is to explore this idea further by directly assimilating the SRR data in a higher resolution model using the National Center for Atmospheric Research Mesoscale Model Version 5 (MM5) four-dimensional variational (4DVAR) data assimilation system. Results of several experiments to evaluate the impact of these data on the prediction of rainfall, track and intensity of Tropical Cyclone Danas (2001) during its initial development are presented.

2. Experiment design

A two-way interactive and triply nested MM5 model (54km x 18km x 6km) is employed in four experiments (Table 1). The initial conditions are derived from the NCEP/AVN analyses. Two experiments are conducted with (NB) and without (CTL) the SRR data (Fig. 1a). Since the initial AVN analysis contains a poor representation of the tropical cyclone vortex, two other experiments (BNT and BT) are conducted with a bogus vortex assimilated into the initial conditions (Zou 2000). All simulations are conducted for 72 h (3 Sep – 6 Sep 2001) during which Danas intensified into a typhoon and made an abrupt turn (Fig. 1b).

To include as much available data as possible but to avoid the spatial correlation for high-resolution data (such as in the 6-km inner domain), the SRR data are directly assimilated in the 18-km domain. The MM5 4DVAR system minimizes the least-squared differences between the SRR observations and the rainfall rates generated by the MM5 model averaged over a 6-h analysis window. The minimization procedure is stopped after 30 iterations.

3. Results

a. Rainfall distribution

Inclusion of the SRR data obviously improves the rainfall prediction, with the BT experiment giving the largest improvement (Fig. 2).

b. Track and intensity

Inclusion of the SRR data improves the track in all the experiments (Fig. 3a), with the BT experiment giving the most significant improvement. The minimum sea-level pressure (SLP) prediction is also the best in the BT experiment (Fig. 3b). In general, experiments with the SRR data produce a more intense tropical cyclone.

References

Hou, S. Q. Zhang, A. M. DaSilva, and W. S. Olson, 2000: Improving assimilated global datasets using TMI rainfall and columnar moisture observations. *J. Climate*, **13,** 4180-4195.

Krishnamurti, T. N., H. S. Bedi, and K. Ingles, 1993: Physical initialization using SSM/I rain rates. *Tellus*, **45A,** 247-269.

Pu, Z., W.-K. Tao, S. Braun, J. Simpson, Y. Jia, J. Halverson, W. Olson and A. Hou, 2002: The impact of TRMM data on mesoscale numerical simulation of supertyphoon Paka. *Mon.Wea.Rev*., **130,** 2448-2458.

Zou, X, and Q. Xiao, 2000: Studies on the initialization and simulation of a mature hurricane using a variational bogus data assimilation scheme. *J. Atmos. Sci*., **57,** 836-860.

TABLE 1. Design of numerical experiments

Numerical expt.	Bogus vortex?	Model initial condition
Control (CTL)	No	NCEP/AVN prediction without TMI SRR
NB	No	NCEP/AVN prediction with TMI SRR
BNT	Yes	NCEP/AVN prediction without TMI SRR
BT	Yes	NCEP/AVN prediction with TMI SRR

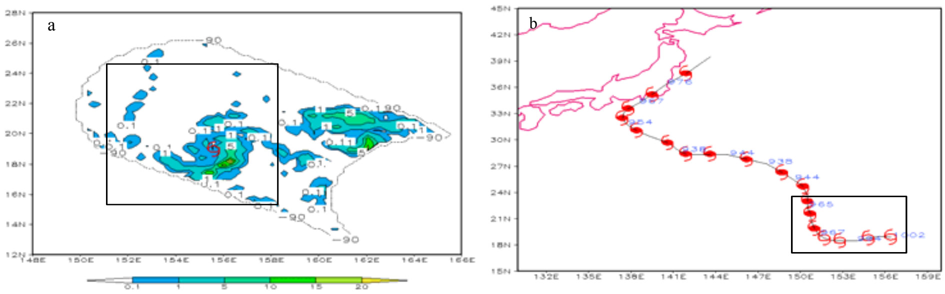

Fig. 1. (a) TRMM/TMI SRR (mm h^{-1}) at 0509UTC-0512UTC on 3 Sep 2001. The "-90" contour indicates the observed area and the SRR data inside the rectangle are assimilated. (b) Track of Danas from 00UTC on 3 Sep 2001 at 12-h intervals. The rectangle indicates the simulation period.

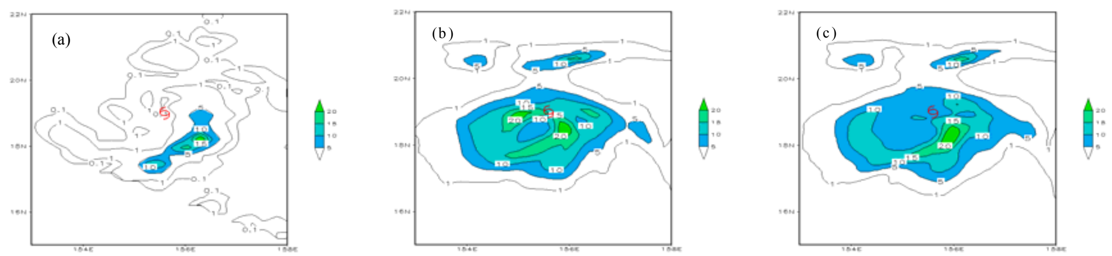

Fig. 2. (a) TRMM/TMI SRR, and simulated SRR in experiment (b) BNT and (c) BT at 0509-0512UTC 3 Sep 2001. Unit: mm h^{-1}.

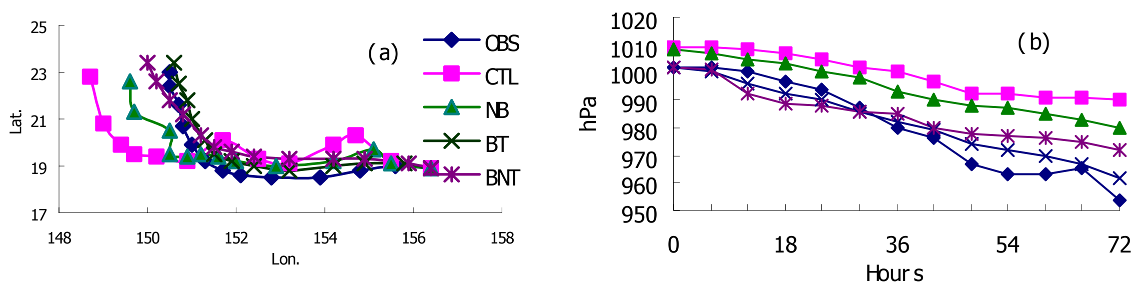

Fig. 3. Observed and predicted (a) tracks and (b) minimum SLP of Danas from 00UTC 3 Sep 2001.

The assimilation of AIRS radiance data at ECMWF

A.P. McNally, P.D. Watts, J. Smith and R. Engelen
European Centre for Medium-range weather forecasts
Shinfield Park, Reading, RG29AX UK

The NASA-AQUA satellite was launched in May 2002 and a subset of the measured radiance data from the Atmospheric Infrared Sounder (AIRS) has been made available to NWP centres since November 2002. The AIRS is a high spectral resolution sounder that potentially provides atmospheric temperature and composition information at a much higher vertical resolution than has been available before. The ECMWF 4DVAR analysis system has been adapted to assimilate the AIRS radiance data. A key element of the assimilation system is a cloud detection scheme that identifies which of the AIRS channels at a particular location are cloud-free and which are contaminated. This approach (rather than the identification of completely clear locations) was chosen to maximize the use of information from the AIRS instrument above the cloud top (e.g. in situations were the scene is covered by low or mid-level cloud with many of the upper sounding channels being unaffected by its presence). The details of the cloud detection scheme are described in *McNally and Watts 2003*. Other elements of the assimilation system (such as bias correction and quality control) are similar to those developed to assimilate radiance data from the operational (low spectral resolution) sensors (i.e. HIRS, AMSUA, AMSUB and SSM/I).

The assimilation system has initially been tuned to be conservative in its use of AIRS data, by assigning relatively large observation errors to the radiances (ranging from 0.6K to 2.0K) and avoiding parts of the spectrum affected by solar radiation and ozone (the latter has significant RT model problems). Despite this conservative approach, the use of AIRS data showed a modest, but consistent positive impact upon the quality of the analysis and forecasting system (figure 1). On the basis of these results the AIRS data were incorporated into the ECMWF operational assimilation system at the end of September 2003. Future development is aimed towards making more extensive use of the AIRS data. For example, the cloud detection scheme is currently rather stringent and could be relaxed to allow more data into the analysis (but may have to be coupled with an estimation of the contribution of the cloud to the radiance signal). Another area where improvement is expected is using more of the information provided by the AIRS spectra. Currently it is not practical to distribute all of the 2378 AIRS channels in near-real-time to NWP centres. However, there are principal component (eigenvector) representations of the full spectra that could convey the information in a very efficient manner (with additional de-noising properties). These are being investigated.

The use of AIRS data to estimate trace gas concentrations is also an active area of research with the initial focus on CO2. Column values (shown in figure 2) are estimated simultaneously within the main 4DVAR analysis system (taking advantage of other observations to constrain temperature and humidity that would otherwise confuse the CO2 signal). Early results are very promising, showing some significant departures from background (climatological) knowledge when and where the atmosphere is clear sufficiently often to allow a meaningful averaging of individual point CO2 estimates.

<u>References</u>

McNally and Watts, 2003 A cloud detection algorithm for high-spectral-resolution IR sounders *QJRMS* **129** pp3411-3423

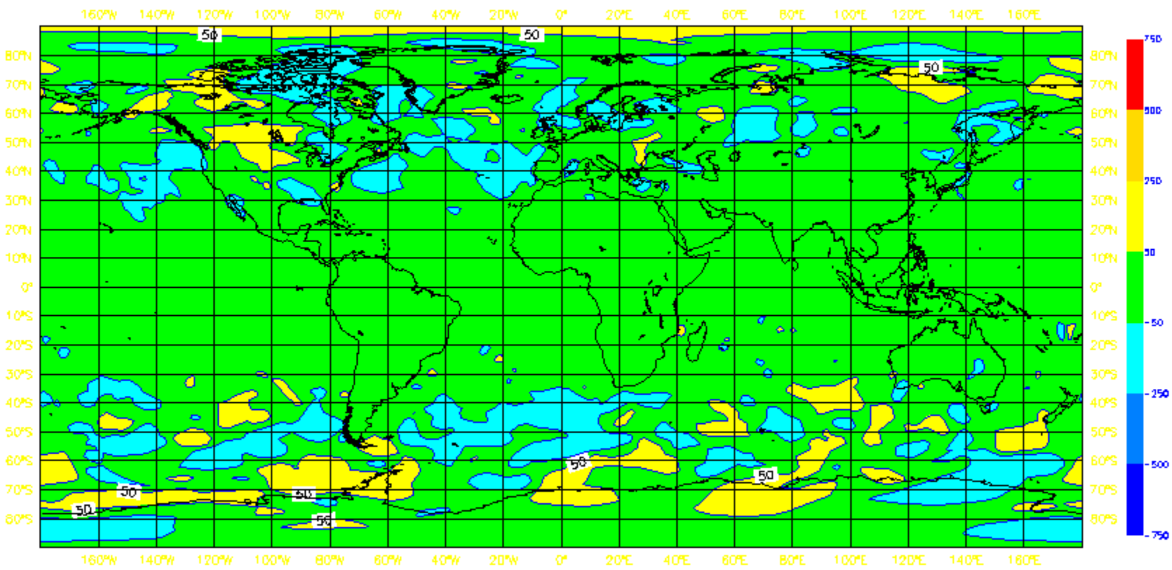

Figure 1 RMS error of day-5 forecasts of 500hPa geopotential , CONTROL system (no AIRS) minus the AIRS system averaged over 40 days (blue shading indicates the use of AIRS reducing forecast errors)

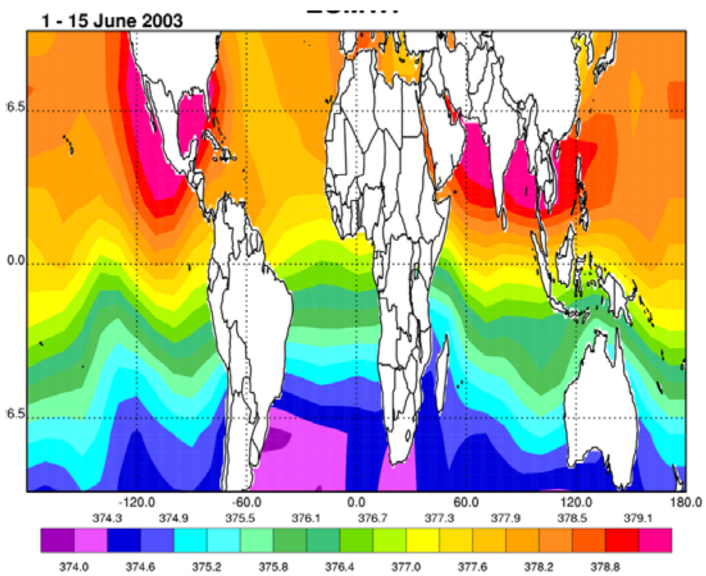

Figure 2 Tropospheric column CO2 estimated within the AIRS assimilation system, averaged over 15 days in June 2003.

Introduction of Vertical Normal Mode Incremental Initialization for a High Resolution Global Model

Hiroyuki Murakami*,Takayuki Matsumura**
***Advanced Earth Science & Technology Organization(AESTO)**
****Numerical Prediction Division, Japan Meteorological Agency**
e-mail:murakami@naps.kishou.go.jp

1 Introduction

The Japan Meteorological Agency (JMA), the Meteorological Research Institute (MRI) and the Advanced Earth Science and Technology Organization (AESTO) cooperate to develop a global climate model, which is called "JMA-MRI Unified Global Model"(Katayama, *et al.*, 2003). Because the model is utilized to investigate the effect of global warming on typhoons through time-slice numerical experiments, balanced initial condition is needed. The JMA also plans to use this model operationally in high resolution with a four-dimensional variational assimilation (4DVAR) system in the future. Even though analysis will be consistent with the model dynamics, it will still contain spurious high-frequency noise if the minimization of cost function in the 4DVAR is performed at lower resolution than the forecast model because model topography is different. Therefore, initialization will still be necessary for high resolution model.

Originally, the JMA-MRI Unified Global Model had a module of nonlinear normal mode initialization (conventional NNMI) (Daley, 1991). However, there was a problem that the computational costs of horizontal structure separation became much higher as a model resolution becomes higher. The time-slice numerical experiments are planned to be conducted with a 20km mesh resolution model. If the conventional NNMI method were used for initialization in such a high resolution, total memory for eigenvalues and eigenvectors becomes several giga bytes. Since it is impractical to carry out the conventional NNMI for high resolution model, a new initialization method is needed.

In order to carry out initialization in the high resolution model, we introduce a vertical normal mode initialization scheme(Bourke and McGregor, 1983) which doesn't require horizontal structure separation. To achieve such a simplified method, incremental nonlinear normal mode initialization(INCNMI) (Ballish, *et al.*, 1992) is also introduced.

2 Incremental normal mode initialization

The INCNMI uses most of the procedures of the conventional NNMI. In the conventional NNMI, the tendencies of the model fields are calculated from analysis. However, in the INCNMI, the tendencies of the model fields are first calculated from the analysis first guess (i.e., the 6-h forecast). And the tendencies of the analysis first guess are then stored in the computer. Next the model tendencies due to the analysis are also calculated. Then, the guess tendency is subtracted from the analysis tendency, which is called "increment". And the increment is passed to the same normal-mode initialization code. After modification, the increment is added to the guess. We introduce the INCNMI into the JMA-MRI Unified Global Model to achieve the following vertical mode initialization.

3 Vertical mode initialization

When primitive equations are linearized by deriving perturbation from basic state, the linearized equations after vertical separation become

$$\frac{\partial \zeta}{\partial t} = -fD - \beta V + N_\zeta,$$

$$\frac{\partial D}{\partial t} = -\nabla^2 \Phi + f\zeta - \beta U + N_D,$$

$$\frac{\partial \Phi}{\partial t} = -\xi^2 D + N_\Phi,$$

where ζ is the vorticity, D is the divergence, Φ is the geopotential, U and V are wind velocities, f is the Coriolis parameter, β is the latitudinal derivative of Coriolis parameter, ξ is the term of equivalent depth of shallow water equation, N mean the non-linear terms.(Bourke and McGregor, 1983)

In the conventional NNMI, these equations are applied to horizontal structure separation for normal mode initialization(Daley, 1991). Bourke(Bourke and McGregor, 1983) proposed an applied initialization scheme for limited area, in which the initialization is implemented in the vertical modes on the assumption that the β can be neglected by the f-plane approximation. As a result, those equations treat only gravitational waves. This suggests high-frequent gravitational waves can be modified without huge matrix calculations of horizontal structure separation.

We apply the above simplification into the JMA-MRI Unified Global Model on the assumption that the neglect of β is allowed because the analysis first guess maintains Coriolis part by introducing the INCNMI.

4 Result

The results to be discussed here is to investigate whether the new initialization can suppress spurious gravity wave oscillations in a low resolution model (T213L40). Data assimilation and forecast experiments were conducted to test the impact of the new initialization.

Figure 1 displays surface pressure variations for the first 24 hours at one grid point. It denotes that without initialization (thin solid curve), there are oscillations with amplitudes of two hPa with periods of only a few hours. Dashed curve denotes the conventional NNMI and bold solid curve denotes the vertical mode initialization with INCNMI (new initialization). With both cases, the spurious waves seem to be well removed. It indicates that spurious gravity waves are suppressed well with the new initialization.

Two data assimilation experiments using the conventional NNMI and the new initialization were conducted for the period of 1-31 July 2002 and 1-31 January 2003. Nine days forecasts were performed for 22 cases from 12UTC 1 July to 22 July 2001 and 15 cases from 8 January to 22 January 2003. The model resolution is T106L40 and assimilation method is 3DVAR. Figure 2 shows the mean forecast error of 500 hPa geopotential height over the global (90 °S-90 °N) averaged for the each cases with respect to the forecast time. This indicates the impact of new initialization for forecast skill is neutral in both July 2002 and January 2003.

The JMA plans to change the conventional NNMI to the new initialization at the same time of operational introduction of semi-Lagrangian integration schemes in October 2004.

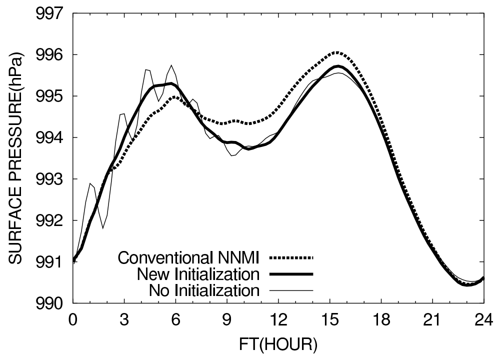

Fig.1 Surface pressures in hPa for a grid point of the foot of Tibet (90 °E,25 °N). Thin solid curve is uninitialized starting analysis. Dashed curve is the conventional NNMI. Bold solid curve is the new initialization.

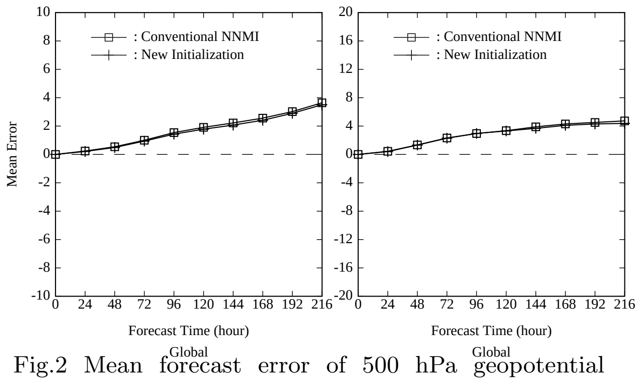

Fig.2 Mean forecast error of 500 hPa geopotential height(m) over the global (90 °S-90 °N). Left: Averaged 22 cases in July 2002. Right: Averaged 15 cases in January 2003. Square curve is the conventional NNMI. Cross curve is the new initialization.

References

Ballish, B., X. Cao, E. Kalnay and M. Kanamitsu, 1992: Incremental Nonlinear Normal-Mode Initialization. *Mon. Wea. Rev.*, **120**, 1723–1734.

Bourke, W. and J. L. McGregor, 1983: A Nonlinear Vertical Mode Initialization Scheme for a Limited Area Prediction Model. *Mon. Wea. Rev.*, **111**, 2285–2297.

Daley, R., 1991: *Atmospheric Data Analysis.* Cambridge University Press, 457pp.

Katayama, K., H. Yoshimura and T. Matsumura, 2003: Development of a 20 km mesh global NWP model on the Earth Simulator. *CAS/JSC WGNE Research Activities in Atmospheric and Oceanic Modelling*, **33**, 0311–0312.

The study of the influence of the tropical cyclones initialization on the forecast of trajectories using the ETA model

A.E.Pokhil, A.D.Naumov, M. Zaychenko

Moscow, Hydrometeorological Research Center of Russia
11-13 Bolshoy Predtechenski Lane, 123242 Moskow,Russia. E-mail: pokhil@mecom.ru

The tropical cyclones (TC) are one of the most dangerous weather phenomena in the Russian Far East. For this reason the study, numerical modelling and forecasting of TCs are extremely important for Russia. The quality of forecast of the motion and evolution of TCs considerably reduces the damage from TC consequences. The result of experimental forecasts performed with the ETA-model (Mesinger F., 1996) has been considered in this article. The model is adapted for the northwest region of the Pacific Ocean. With this model experimental forecasts have been done for the situations with the most remarkable typhoons of last seasons. The input data for the ETA-model were the objective analysis at 00 h UTC of the Russian Hydrometeorological Centre (RHMC), and for updating lateral boundary conditions the fields from the spectral model of RHMC with 6-h resolution were used (Pokhil A.E., Naumov A.D., 2003).

For a better forecast of the TC motion accurate definition of the TC initial location is very important. The accuracy of the definition of the TC centre is estimated in (Naumov A.D. and Nikolaeva A.V., 2003) for the current variant of the model. The errors in 46 sample cases constituted 134 km in the average. This error was significantly reduced using the vortex initialization procedure. An artificial axially symmetric vortex given by equations (1) or (2) is superimposed on the wind field (obtained from the objective analysis) at the initial moment. We considered the profiles (1, 2) of the wind velocity tangential component:

$$V(r) = Vm\frac{r}{Rm}\exp\left[\frac{1}{b}\left(1-\left(\frac{r}{Rm}\right)^{b}\right)\right] \quad , \qquad (1)$$

$$V(r) = Vm\frac{r}{Rm}\frac{3}{\left[2+\left(\frac{r}{Rm}\right)^{3}\right]} \quad , \qquad (2)$$

where r - distance from the vortex centre; V_m - maximum of the tangential component of the wind velocity; R_m - distance at which V_m is reached; b - a parameter determining the degree of the decrease of the wind velocity tangential component in the radial direction.

The maximum velocity is got from synoptic telegrams. Its radius is assumed to be equal to 3 grid steps. The following conditions are used:

1) The artificial vortex centre is located in the point of the TC centre defined from the satellite data. Thus the error of the TC centre initial location is comparable with the grid step.

2) The area of the artificial vortex in the current version of the model is equal to 30 grid steps, i.e. is about 1000 km.

3) On the boundaries of the artificial vortex the wind velocity values equal the objective analysis wind velocity values.

The initial field of the geopotential is obtained through the solution of the balance equation. This procedure is performed for the 5 lower levels: 1000, 850, 700, 500 and 400 hPa. This initialization provides good accuracy when determining the TC centre location. When specifying initial fields in the neighbourhood of the TC, it is performed in a separate block during the preparation of input data for the ETA-model.

The influence of the initialized vortex structure on the forecast of the real TC motion has been studied. (Pokhil A.E. and Polyakova I.V., 1994) shows that the way of specifying the wind velocity initial field in a model vortex plays a significant role in the motion of this vortex in the surrounding stream. It was necessary to study which kind of the initialized vortex reflects the structure of real TCs best.

To estimate the influence of the initialization way on the behaviour of a real TC a numerical experiment has been performed with the TC Halong, which was passing in the northwest of the Pacific from 7 to 16 July 2002. It reached a hurricane stage with pressure at the centre 945 hPa and the maximum velocity of wind about 90 knots. The change of the TC behaviour has been studied for several algorithms of the initial vortex restoration simulating the TC in the objective analysis fields according to formula (1) at b=1.0; 1.5; 2.0. Initial fields with initialization at b=1.0 and the forecast for 24 and 48 h reflect the real situation well. We have obtained that for the considered synoptic situations the change in trajectories with the change of the initialization way is less than 10-15 %. However more detailed study in this direction is necessary.

References

1. Mesinger F., 1996**:** Improvements in quantitative precipitation forecasts with the ETA regional model at the National Centers for Environmental Prediction. Bull. Amer. Met. Soc., 77, No 11.
2. Pokhil A.E., Naumov A.D., 2003: Using the ETA-model for calculating the evolution and motion of pairs of tropical cyclones in the Pacific. Meteorology and Hydrology, No. 6.
3. Pokhil A.E., Naumov A.D., 2003**:** Analysis of the evolution and motion of tropical cyclones on the basis of calculations using the ETA model and satellite data . -CAS/JSC Working Group on numerical experimentation. Research activities in atmospheric and oceanic modelling. Report N 33, April, WMO/TD-N 1161.
4. Naumov A.D., Nikolaeva A.V., 2003: Using a regional ETA model for forecasting tropical cyclone tracks from data of the Hydrometeorological Scientific Research Center of Russia. Meteorology and Hydrology., 2003, No. 10.
5. Pokhil A.E., Polyakova I.V., 1994: The influence of interactive vorticities on their movement. Meteorology and Hydrology., 1994, No. 7.

USE OF TMI AND SSM/I DATA IN THE JMA OPERATIONAL MESO ANALYSIS

Yoshiaki Sato*, Yoshiaki Takeuchi, Toshiharu Tauchi

Japan Meteorological Agency, Tokyo, Japan

The Japan Meteorological Agency has been operating a Meso-Scale Model (MSM) with 4D-VAR data assimilation system (Meso 4D-VAR). This model is utilized for very short range rainfall forecast to mitigate natural disasters. Although the Meso 4D-VAR brought considerable improvement in the precipitation forecasts of MSM, it still does not have enough accuracy to predict heavy rainfall quantitatively. It needs not only to improve MSM and Meso 4D-Var but also to introduce new observations.

An observational system experiment (OSE) for both rain rates (RR) and total column precipitable water (TCPW) retrieved from Tropical Rainfall Measuring Mission (TRMM) Microwave Imager (TMI) and Special Sensor Microwave/Imager (SSM/I) was performed. To retrieve both RR and TCPW, the method developed by Takeuchi and Kurino (1997) was employed.

A result of the OSE is shown in Fig. 1. The analysis date is 00UTC 25 Aug. 2003. Without TCPW assimilation, a water vapor concentrated area was analyzed over the East China Sea (Fig.1b). However TCPW observation did not show the concentration (Fig 1a). With TCPW assimilation, the high humid area was removed (Fig.1c) and the analyzed field showed good correspondence with the observation. Forecast experiments using MSM from these initial conditions were performed in this case. Radar observation showed that torrential rain occurred at the northern part of Kyushu Island after 18 hours (Fig 1a'). Without TCPW assimilation, a convective system was developed over the East China Sea right after the start of forecast and it moved toward the southern part of Kyushu Island (Fig.1b'). With TCPW, development of the convective system was delayed and heavy rain was predicted at the northern part of Kyushu Island (Fig.1c'), corresponding with the radar observation.

* *Corresponding author address:* Yoshiaki SATO, Numerical Prediction Division, Forecast Department, Japan Meteorological Agency, 1-3-4, Otemachi, Chiyoda-ku, Tokyo 100-8122, Japan; e-mail: y-sato@met.kishou.go.jp

To estimate the total effect of the RR and TCPW, an OSE was performed for two weeks starting from 3 Jun. 2003. Considering the real time operation, TMI and SSM/I data received after the cut-off time were not used in the OSE. Meso Analysis was performed cyclically using those additional data. Forty eight forecasts were performed and compared with operational ones, in which the satellite data were not assimilated.

The threat scores of weak (1mm/3hour) and moderate (10mm/3hour) rain over Japan are shown in Fig. 2. The both threat scores showed positive impact in the rainfall forecast after 12 hours forecast, while they were showed almost neutral up to 9 hours forecast. This result can be explained by that the water vapor field over ocean was improved with the additional data and it needed time to flow over Japan islands. In the operational Meso Analysis, radar data are used and they adjust rainfall field to radar observations. Therefore, no remarkable differences are seen in the threat scores in the first half of the forecast period.

The RMSEs for 500 hPa height (Z500) and 850 hPa temperature (T850) against upper air sounding data are shown in Fig. 3. RMSE for Z500 was slightly improved after 12 hours forecast and T850 was improved from the initial time. RR and TCPW assimilation may affect initial condition of thermodynamical field. Besides the modification of water vapor field changes the location where convection develops, and improved the dynamical field. Undoubtedly, the introduction of those data brought positive effect in MSM forecast.

With the results, JMA decided to use the data in operational Meso Analysis. It has started from 00UTC 15 Oct. 2003.

References:

Takeuchi, Y and T. Kurino, 1997: "Document of algorithm to derive rain rate and precipitation with SSM/I and AMSR," Algorithm description of PIs for SSM/I and ADEOS-II/AMSR, *2nd AMSR Workshop,* 61-1 – 61-9.

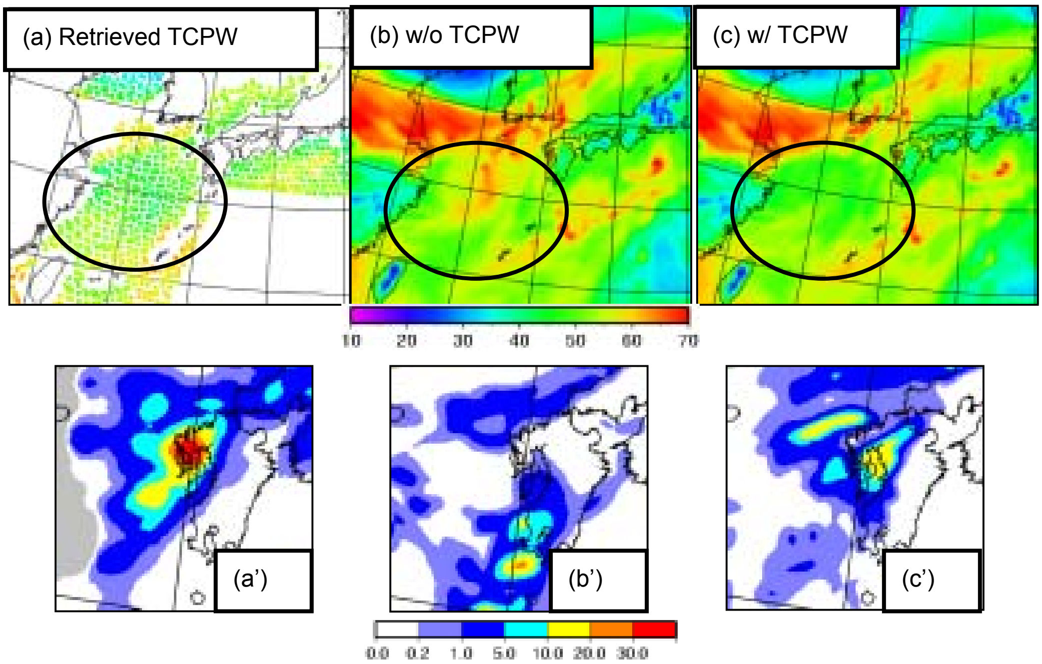

Fig.1 (a) Retrieved TCPW at 00UTC 25 Aug. 2003 from TMI and SSM/I. (b) Analyzed TCPW field at the same time without assimilating TCPW data. (c) Same is in (b) but with TCPW assimilation. (a') 3-hour rain at 18UTC 25 Aug. 2003 estimated by radar observation. (b') 3-hour rain forecast after 18 hours from the initial condition (b). (c') Same is in (b') but from the initial condition (c).

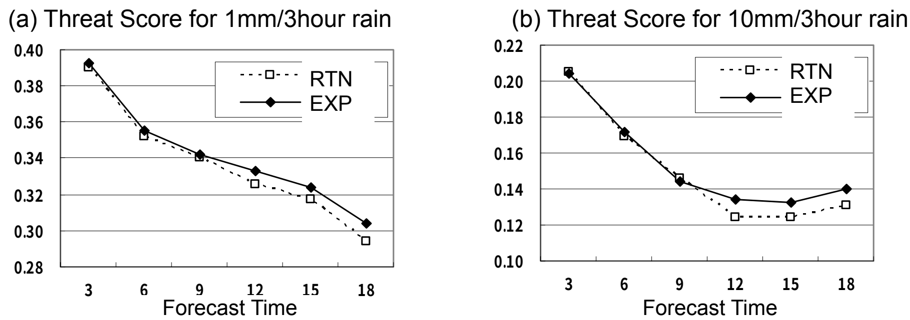

Fig. 2 The threat scores for weak (1mm/3hour) and moderate (10mm/3hour) rainfall forecasts in the two weeks starting from 3 Jun. 2003. RTN means the operational forecast and EXP means the OSE forecast.

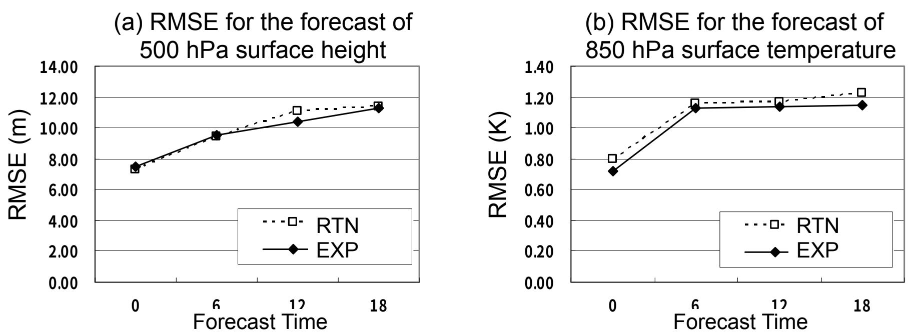

Fig. 3 RMSE of the operational (RTN) and OSE (EXP) forecast against upper air sounding data in the two weeks starting from 3 Jun. 2003.

Impacts of Radial Wind Measured by Doppler Radar and GPS-derived Water Vapor on Numerical Prediction of Precipitation

[1]Hiromu Seko, [2]Tadashi Tsuyuki, [2]Takemasa Miyoshi
[1]Meteorological Research Institute, Tsukuba, Japan
[2]Japan Meteorological Agency, Tokyo, Japan

1. Introduction

Because summer thunderstorms sometimes cause heavy rainfall that is particularly hazardous in urban areas, the accurate forecast of the thunderstorms has been desired. To predict the precipitation more accurately, the variational assimilation systems are developed by the Japan Meteorological Agency (JMA).

On 21 July 1999, a thunderstorm was generated in Tokyo south from the Baiu front and caused the heavy rainfall, of which the hourly rainfall exceeded 100 mm/hour. In general, thunderstorms are generated by the convergence of the low-level humid airflow. Therefore, the radial wind (RW) of Doppler radar and GPS precipitable water vapor (PWV), which have the information of the convergence and humidity, are expected to improve the forecast when they are used as assimilation data.

In this study, the analyzed fields are obtained by 3-dimensional assimilation system (JNoVA0) for the Non-hydrostatic Model (NHM) of JMA (Miyoshi 2003), and the impact of the RW and PWV data was investigated by comparison between the observed and the simulated rainfall fields.

2. Assimilation data

In this study, the RW data that was observed by Narita and Haneda radars, which are about 50km northeast of Tokyo and in the southeastern Tokyo, were used. Because the number of RW data was much larger than that of the model grids, a "super observation method" was used; RW data from the radar were interpolated onto the horizontal grid by a Cressman scheme. Simulated RW at interpolated RW data points were interpolated from the NHM grid point values by using the weight of the radar beam intensity in the vertical direction and a Cressman interpolation in the horizontal direction. The radar beam intensity was assumed to have a Gaussian distribution. As for the GPS PWV data, PWV estimated from the GPS Earth Observation Network (GEONET) data of Geographical Survey Institute (GSI) was used. The mean of horizontal interval of GEONET is about 25 km and the time resolution of PWV data is 5 minutes.

3. Tangential component distribution of analyzed wind

At first, we explain how tangential wind was changed by the assimilation of RW data. Figure 1 shows the distribution of the radial wind and tangential wind of the elevation angle of 0.7 degree. The observed radial and tangential winds were estimated from the horizontal wind observed by Narita and Haneda radars by the dual Doppler radar analysis. In the northern part of the Dual analysis region, the northwesterly inflow expanding eastward and westward was observed (Fig. 1a). When the radial wind of two radars was used, the analyzed wind fields were very close to observed ones (Fig. 1c). When only the radial wind of Haneda radar was used, the radial wind was similar to the observed one and the tangential wind that expanded eastward and westward was obtained (Fig. 1d). The comparison of the tangential wind indicated that the RW data changed the tangential wind to one similar to the observed one even if RW data of single radar was used.

4. Impact of radial wind of Doppler radar and GPS-derived Water Vapor

Comparisons between forecasted rainfall regions with and without the assimilation help define the impacts of RW and PWV data. When the assimilation was not performed (Fig. 2a), the rainfall region did not move southward and the thunderstorm was not generated in Tokyo. When the RW and PWV data were assimilated, the low-level inflow became more humid, and low-level northerly flow was reproduced in the north of Tokyo (Fig.2 b). This northerly flow intensified the low-level convergence and the thunderstorm was generated near Tokyo (red circles in Fig. 2b). For this rainfall event, the assimilation of RW and PWV data improved the precipitation prediction.

---

*Corresponding author address: Hiromu SEKO, Meteorological Research Institute, 1-1 Nagamine Tsukuba Ibaraki 305-0052, Japan: e-mail: hseko@mri-jma.go.jp

Acknowledgments

The authors thank Dr. K. Akaeda of JMA, Mr. Y. Tanaka of MRI and the staff of GSI for providing Doppler radar data, the decode programs of the Doppler data and GPS data.

References

Miyoshi Takemasa, 2003: Development of 3D-Var Assimilation System (JNoVA0), Bettsusatsu-houkoku, NPD/JMA, 49,148-155.

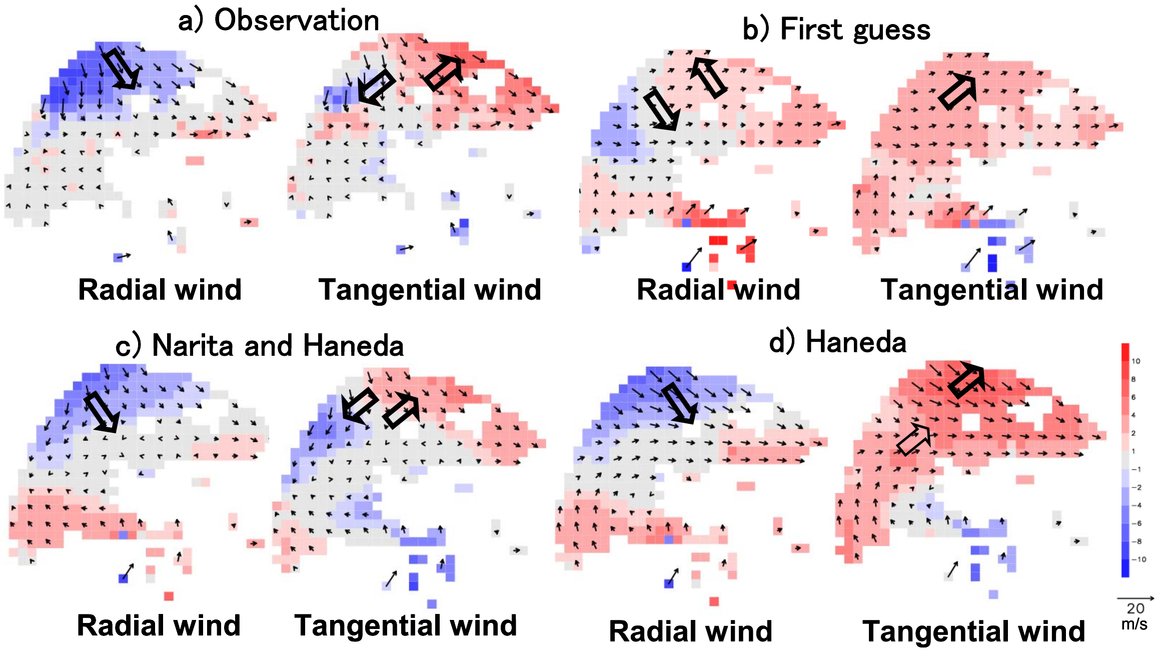

Fig. 1 Distribution of the radial and tangential wind of the elevation angle 0.7 deg. (a) Observed wind estimated from the horizontal wind obtained from Narita and Haneda radar data by the dual Doppler radar analysis. (b) First guess wind fields. (c) and (d) Analyzed radial and tangential wind obtained from the analyzed horizontal wind.

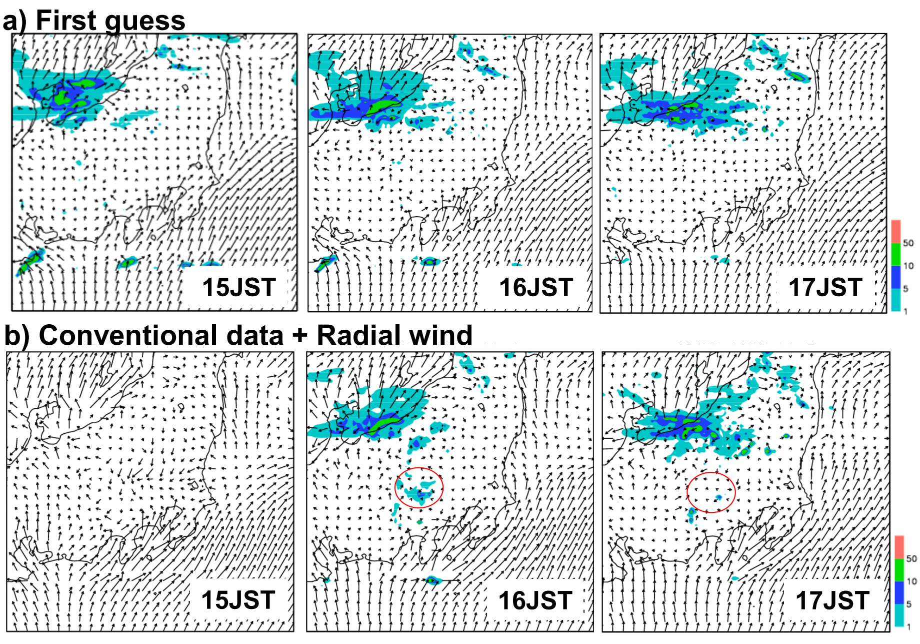

Fig. 2 Rainfall region simulated from the initial fields (a) without assimilation and (b) with assimilation of conventional data, radial wind of Haneda and Narita radars and GPS-PWV data.

Operational Implementation of the JMA Regional Four-Dimensional Variational Data Assimilation System

Toshiki Shimbori* and Ko Koizumi

Numerical Prediction Division, Japan Meteorological Agency

Tokyo 100-8122, Japan

The four-dimensional variational data assimilation (4D-Var) system for the meso-scale model (MSM) of Japan Meteorological Agency (JMA) has been operational since March 2002 (Ishikawa and Koizumi, 2002). In June 2003, JMA has also implemented the 4D-Var system for the regional spectral model (RSM) instead of the three-dimensional optimal interpolation system with a physical initialization (hereafter called 3D-OI). To support a short-term forecast up to 2 days, RSM makes forecasts over East Asia area with 20 km horizontal resolution and 40 vertical levels up to 10 hPa and also provides the lateral boundary condition for MSM. The 4D-Var system for RSM has 6-hour assimilation windows, i.e. ±3 hours of the analysis time. Assimilated data are SYNOP, TEMP, Wind-Profiler, SHIP, BUOY, AIREP, AMW and Radar-AMeDAS precipitation analysis.

In order to evaluate the performance of the 4D-Var system for RSM in the operational environment, 6-hour forecast-analysis cycle experiments were performed for one-month period of June 2002 and January 2003. 51-hour forecasts were made twice a day (00 and 12 UTC initials). The root mean square error (RMSE) and the mean error of 500 hPa geopotential height for June 2002 are shown in Fig. 1. The RMSE of the 4D-Var system is smaller at every forecast time, which indicates that the 4D-Var has better performance than the 3D-OI system. On the other hand, the mean error that represents the bias of RSM does not differ so much in both systems. The threat and bias scores of precipitation forecasts over 1 mm/6 hour for June 2002 are shown in Fig. 2. The threat score of the 4D-Var surpasses that of the 3D-OI system for every forecast time. On the other hand, the change of the bias score is small. The errors and scores for January 2003 show similar results (figures not shown). An example of precipitation forecasts is shown in Fig. 3. In this case, heavy rain was observed at Tanegashima and Yakushima Islands, south of Kyushu. The forecast from the 4D-Var system shows a good agreement with the observation, while that from the 3D-OI system failed to predict the heavy rain.

* E-mail: shimbori@met.kishou.go.jp

Reference

Ishikawa, Y. and K. Koizumi, 2002: One month cycle experiments of the JMA mesoscale 4-dimensional variational data assimilation (4D-Var) system. Research Activities in Atmospheric and Oceanic Modelling, No. 32, WMO/TD-No. 1105, 01.26-01.27.

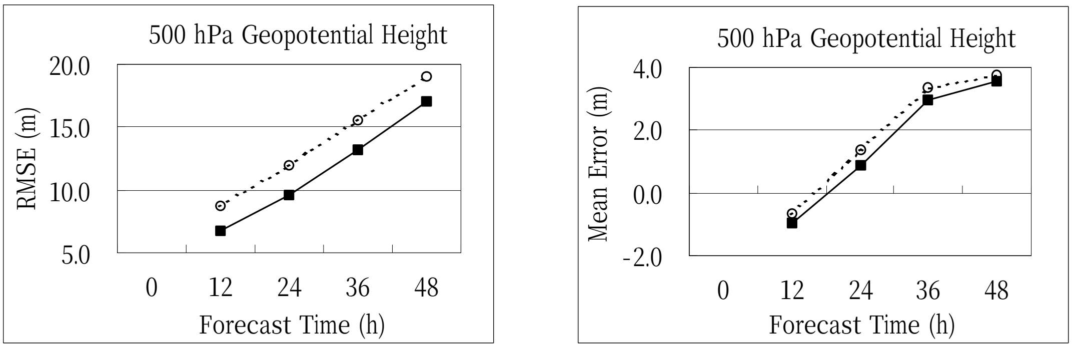

Fig. 1: Root mean square and mean errors of 500 hPa geopotential height against initialized analysis (1-30 June 2002), with 4D-Var (solid) and 3D-OI (dashed).

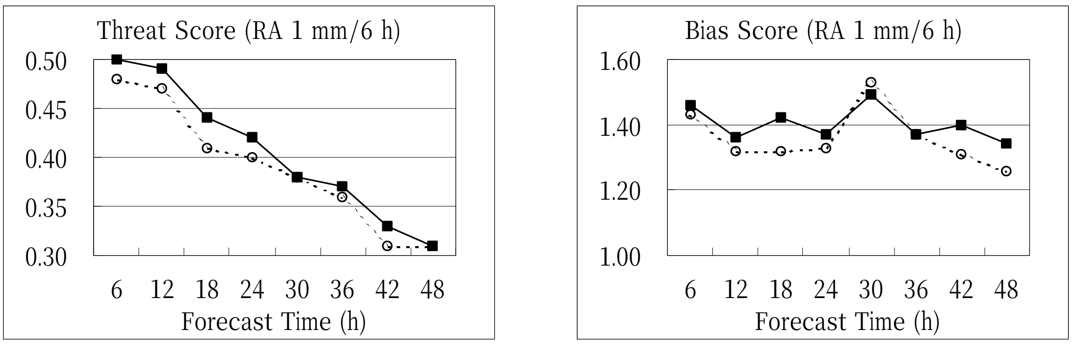

Fig. 2: Threat and bias scores of 1 mm/6 hour against 40 km-averaged Radar-AMeDAS precipitation analysis (1-30 June 2002), with 4D-Var (solid) and 3D-OI (dashed).

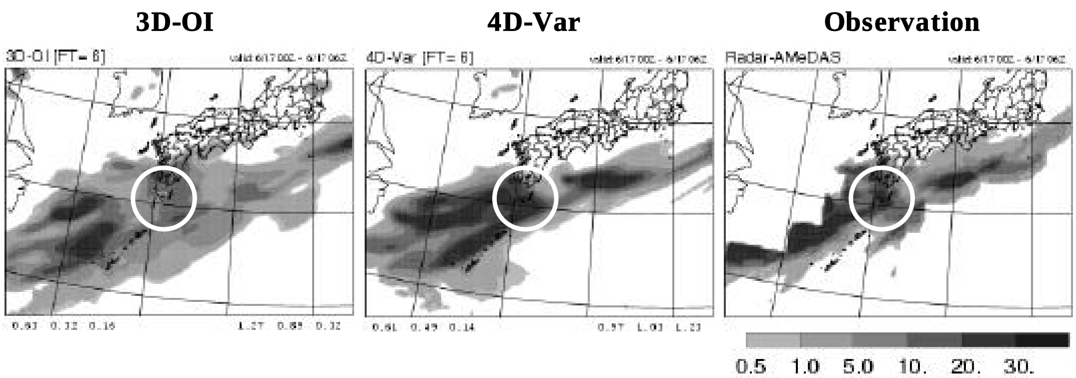

Fig. 3: 6-hour precipitation in 00-06 UTC 17 June 2002 (initial times are 00 UTC 17 June 2002).

ENSEMBLE DISPERSION SPECTRA AND THE ESTIMATION OF ERROR STATISTICS FOR A LIMITED AREA MODEL ANALYSIS

Simona Ştefănescu [1] , Loïk Berre [2]

1. Introduction

Deriving background error statistics can be done using an ensemble of perturbed assimilation systems. Houtekamer et al. (1996) combined two complementary approaches into a system simulation experiment, namely an ensemble prediction based on a perfect-model approach, for which only the observations that enter in the assimilation cycle are randomly perturbed, and model sensitivity experiments. The analysis ensemble approach was also implemented at the ECMWF (Fisher, 1999) and Meteo-France (Belo Pereira, 2002).

In the present study, the ensemble approach is used to sample the forecast error covariances to be used in a 3D-Var data assimilation for the limited area model ALADIN. A generalized formulation of this 3D-Var is considered, in which the analysis of the coupling model, namely ARPEGE, is included as an additional source of information (Bouttier, 2002). This is related to the idea of relying on the "fresh" ARPEGE analysis for the large scales, while still extracting the small scale information of the ALADIN background. The evolution of dispersion spectra in the perfect-model framework has been investigated. The ARPEGE/ALADIN model differences have been also evaluated, and a decomposition of them is proposed. Finally, the implications for the specification of the error statistics in the generalized formulation of the ALADIN 3D-Var data assimilation are pointed out. A comparison with the statistics derived through the NMC method has been carried out too.

2. Contributions to the evolution of dispersion spectra in a perfect-model framework

From the ARPEGE ensemble of perturbed assimilation cycles, it is possible to run the operational ALADIN limited area system (currently in dynamical adaptation mode): this provides an ensemble of limited area states, whose evolution of dispersion can be studied.

The effect of ARPEGE analysis is to reduce the error variance, especially in the large scales (see figure 1). The reduction of the ARPEGE first guess variance is about 30 percents for the wavenumber 1.

After applying a digital filter initialization (DFI), a reduction of the error variance for ARPEGE analysis and first guess, especially in the small scales, has been observed. This can be explained by the fact that DFI removes some unbalanced components of the error variance, namely the structures artificially created in the small scales by the horizontal interpolation of the ARPEGE fields into the ALADIN grid.

Compared with the ARPEGE 6h forecast, the effect of ALADIN 6h forecast is to increase the error variance in the small scales. The ALADIN 6h forecast and ARPEGE 6h forecast error variance curves start to depart significantly at wavenumbers greater than 13-17, i.e. corresponding to length scales smaller than 220-170 Km, as can be seen from figure 2. This means that the limited area model builds up its own structures beyond these wavenumbers. The smaller errors of ARPEGE (than those of ALADIN) that are suggested in the small scales can be understood on one hand, knowing its low resolution and the effect of diffusion, but it can also be seen as a paradox on the other hand, as we would expect that the higher resolution model (ALADIN) should give a better solution in the small scales.

3. Model difference evaluation and decomposition

We have calculated the differences between the ARPEGE and ALADIN models, when these two models are subject roughly to the same initial state. The potential of these model differences is to give informations about some of the involved model errors.

The ARPEGE/ALADIN model differences appear to be relatively small scale compared with the differences that are related to the initial condition perturbations, but there are also some significant contributions in the large scales. This suggests that the model differences arise not only from the differences in resolution, but possibly also from the coupling inaccuracies and from the interactions between the small and large scales. One may wonder therefore if it could be possible to distinguish these different possible contributions.

A parameter α has been defined, in order to estimate the part of the model differences that is related to the resolution differences. α is defined as the percentage of ALADIN dispersion that is unrepresented by ARPEGE:

$$\alpha = [var(ald06) - var(arp06i)]/var(ald06) \quad (1)$$

[1] National Institute of Meteorology and Hydrology, Sos. Bucuresti-Ploiesti 97, sector 1, 013686 Bucharest, Romania, e-mail: simona.stefanescu@meteo.inmh.ro

[2] Meteo-France CNRM/GMAP, 42 av. G. Coriolis, 31057 Toulouse Cedex 01, France, e-mail: loik.berre@meteo.fr

Further, the model differences variance $var(\epsilon^m)$ can be decomposed as follows:

$$var(\epsilon^m) = \underbrace{\alpha \cdot var(\epsilon^m)}_{var(\epsilon^{ss})} + \underbrace{(1-\alpha) \cdot var(\epsilon^m)}_{var(\epsilon^{ls})} \tag{2}$$

$var(\epsilon^{ss})$ corresponds to the small scale structures that are represented by ALADIN and not by ARPEGE: they may be interpreted as some ARPEGE model errors, with respect to the truth at the ALADIN resolution.

The residual $var(\epsilon^{ls})$ corresponds to some large scale structures, that are related e.g. to some coupling inaccuracies and to some small scale/large scale interactions. In the future, a refined decomposition of this residual could be obtained by comparing some global and limited area models with similar resolutions, and also by comparing some global models with different resolutions.

The decomposition of the ARPEGE/ALADIN model differences variance into small scale and large scale parts is represented in figure 3.

4. Implications for the specification of the error statistics in the generalized formulation of the ALADIN 3D-Var

The variances of the decomposed model differences have been added to the respective dispersion variances of the ARPEGE analysis and of the ALADIN background (see figure 4). A multiplying factor 2 is used for these model difference variances, to be consistent with the corresponding factor 2 that is implicit in the variance estimates provided by the ensemble of analyses with a perfect model.

The variance of the small scale structures that are unrepresented by the ARPEGE model has been added to the variance of the ARPEGE analysis dispersion. This increases strongly the small scale dispersion, while leaving the large scale dispersion mainly unchanged.

The variance of the large scale model differences may be added to the variance of the ALADIN background dispersion, if they are interpreted as being caused by ALADIN (due to coupling errors for instance); this increases mostly the large scale dispersion.

The comparison between the two final dispersion spectra suggests that in the large scales, the ARPEGE analysis errors are smaller than those of the ALADIN background, while the reverse holds in the small scales.

This ensemble approach, based on some perturbed assimilation cycles and model differences, appears therefore to be a good framework for the evaluation of the error statistics that are involved in the generalized formulation of the ALADIN 3D-Var.

References

Belo Pereira M., 2002: Improving the assimilation of water in a NWP model. Reports for ALATNET Newsletters 4 and 5.

Bouttier F., 2002: Strategies for kilometric-scale LAM data assimilation. Hirlam workshop report on variational data assimilation and remote sensing 21-23 January 2002, Helsinki, p.9-17.

Fisher M., 1999: Background error statistics derived from an ensemble of Analyses. ECMWF Research Department Technical Memorandum No. 79, September 1999, 12pp.

Houtekamer et al., 1996: A system simulation approach to ensemble prediction. Mon. Wea. Rev., 124. 1225-1242.

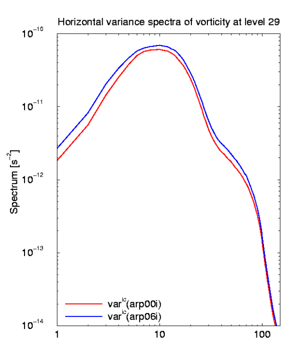

Figure 1: Dispersion spectra related to the initial condition perturbations for initialized ARPEGE analysis and first guess fields

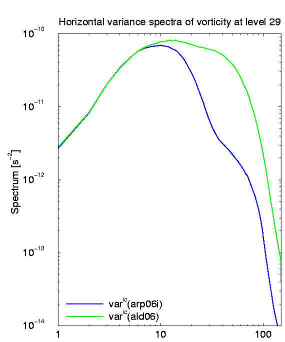

Figure 2: Dispersion spectra related to the initial condition perturbations for initialized ARPEGE first guess and ALADIN background fields

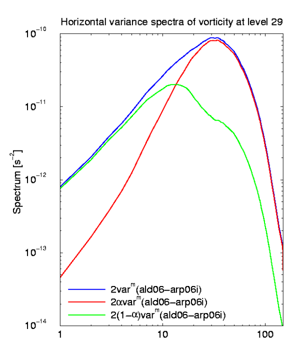

Figure 3: Decomposition of initialized ARPEGE first guess / ALADIN background differences variance

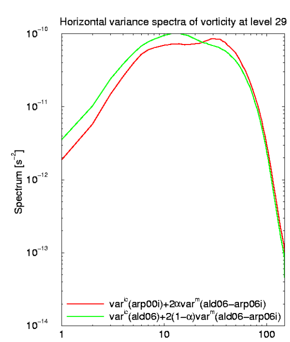

Figure 4: The final dispersion spectra for initialized ARPEGE analysis and ALADIN background fields

Assimilation of SSM/I and TMI Total Column Precipitable Water Data into the JMA Global 3D-Var Assimilation System

Toshiharu Tauchi*, Yoshiaki Takeuchi, Yoshiaki Sato
Numerical Prediction Division, Japan Meteorological Agency
1-3-4 Otemachi, Chiyoda-ku, Tokyo 100-8122, JAPAN
e-mail:ttauchi@naps.kishou.go.jp

In order to improve global water circulation forecast, it is essential to prepare accurate model initial fields, especially for water vapor. The Japan Meteorological Agency (JMA) has been trying to introduce total column precipitable water (TCPW) data, which can be retrieved from Microwave Radiometer, into the global 3D-Var assimilation system.

An observation system experiment (OSE) for TCPW from SSM/I on DMSP -13, 14 and 15 and TRMM/TMI was conducted. Predetermined look-up tables for SSM/I and TMI were used to retrieve TCPW (Takeuchi and Kurino 1997). Some biases between the satellites were corrected before OSE.

In the preliminary experiment, excessive precipitation was appeared in the tropics due to systematic difference between the retrieved TCPW and the guess TCPW of the JMA global model (GSM) as shown in Fig. 1a. To remove the undesirable difference, a bias correction was applied to the retrieved TCPW (Fig. 1b).

With the bias corrected TCPW, an OSE was performed for the period of 1-31 July 2003. Fig. 2a shows the difference in monthly mean analyzed TCPW fields between the test with TCPW assimilation and control. The monthly mean TCPW increased mainly over Indonesia and Northern Atlantic Sea, and decreased over the Arabian Sea. It affected lower layer temperature (Fig. 2b). Figure 3 shows the RMSE for 850 hPa temperature (T850) forecast against radio-sonde observation in the tropical region (20S-20N). The decrease of RMSE up to 4 days forecast is remarkable.

Although the T850 score against radio-sonde observation was improved, a model-originated cooling bias in the lower troposphere (Nakagawa 2003) resulted in the degradation of forecast scores against initial field. To solve the problem, we are investigating the detail mechanism of the forecast degradation in the TCPW assimilation.

References:

Takeuchi, Y and Kurino, T, 1997: "Document of algorithm to derive rain rate and precipitation with SSM/I and AMSR," Algorithm description of PIs for SSM/I and ADEOS-II/AMSR, 2nd AMSR Workshop, 61-1 - 61-9.

Nakagawa, M, 2003: Development of a cumulus parameterization scheme of the operational global model at JMA, CAS/JSC WGNE Res. Act in Atmos. Ocea. Model.

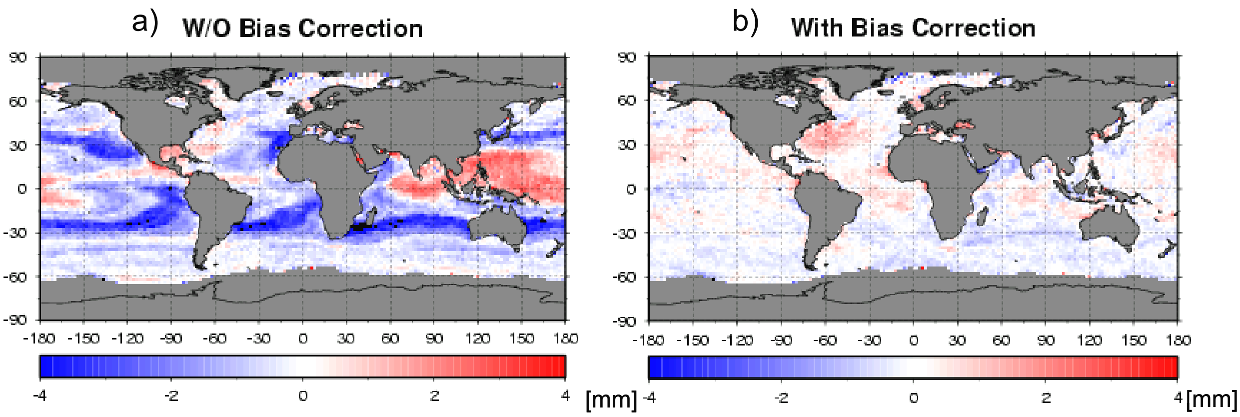

Fig.1: Monthly mean TCPW difference between the guess of global model and the retrieval, a) Without the bias correction and b) With the bias correction. The period is 1-31 July 2003.

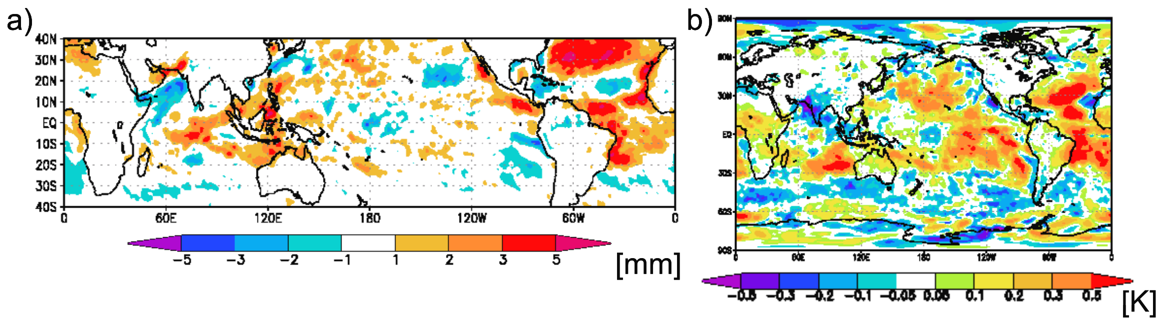

Fig. 2: a) Difference of monthly mean analyzed TCPW between the test with TCPW assimilation and the control. b) Same as is a) but for temperature at 850 hPa. The period is 1-31 July 2003.

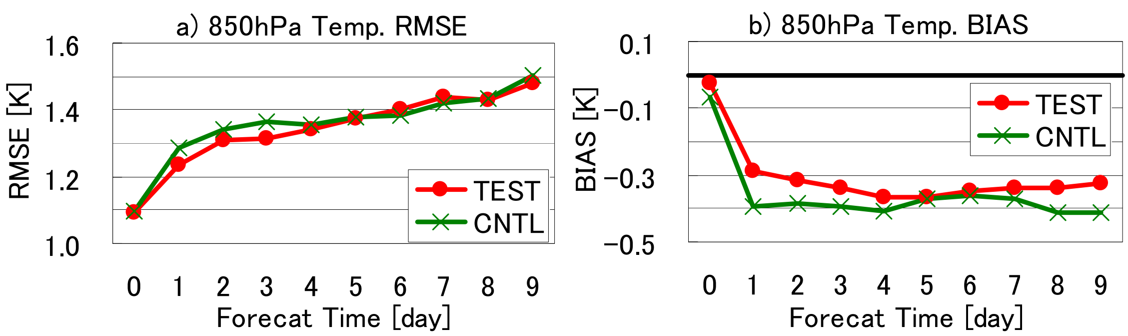

Fig. 3: a) RMSE for 850 hPa temperature forecast in tropical area against radio-sonde observation. b) Same as is a) but for mean error.

Impact of GMS-5 Cloud-drift Winds on the Track Prediction of Tropical Cyclones

DONGLIANG WANG*, XUDONG LIANG AND YIHONG DUAN
Shanghai Typhoon Institute, China Meteorological Administration, Shanghai, China
*Email: wangdl@mail.typhoon.gov.cn

1. Introduction

The assimilation of cloud-drift winds into numerical-weather-prediction models for tropical cyclones has been done in the past using some simple schemes such as the three-dimensional optimum interpolation method (e.g. Goerss et al. 1995; Brian et al. 2001). Such assimilations generally resulted in some reductions in the mean track errors. Recently, Xiao et al. (2002) examined the impact of satellite-derived winds on the prediction of a mid-Pacific cyclone using a more sophisticated tool – the four-dimensional variational (4DVAR) data assimilation method. They demonstrated that the data only had a slight positive impact on the prediction, although their study was limited to only five time-lag experiments. The objective of this study is to carry out a set of 4DVAR experiments to assess further the impact of cloud-drift winds from the Geosynchronous Meteorological Satellite 5 (GMS-5) on the initial conditions and track predictions of tropical cyclones (TCs) in the western North Pacific (WNP).

2. Cloud-drift wind dataset and assimilation methodology

The data assimilated in this paper are derived from GMS-5 infrared and water vapor imageries and provided by the China National Satellite Meteorological Center. About 70% of the multispectral winds are observed above 400 hPa, and 50% of the data are between 200 and 300 hPa.

Experiments are carried out using the nonhydrostatic National Center for Atmospheric Research Mesoscale Model Version 3.3 (MM5) and its 4DVAR system. A 6-h assimilation window is used to incorporate the cloud-drift winds at the initial time and 6 h later. Previous statistics suggest that the error in the upper-troposphere cloud-drift winds is ~ 6 m s^{-1}. Therefore, a simple quality control similar to the first-guess check in the ECMWF system is used here: any cloud-drift wind with a difference from the MM5 original analysis > 3 times the error, i.e. 18 m s^{-1}, is rejected.

Twenty-two cases are examined for 8 different WNP TCs in 2002. Forecasts up to 48 h are performed with the original and 4DVAR-assimilated initial conditions.

3. Results

An example of the impact on the initial conditions is presented for the case of Phanfone (Fig. 2). The largest adjustment through assimilation occurs south of the typhoon center (30^{O}N, 138^{O}E). The original MM5 analysis produces inaccurate south to southwesterly winds (Fig. 2b). Assimilation of the cloud-drift winds apparently brings back the observed anticyclonic circulation (Fig. 2c) so that the flow in this area is very close to that observed (Fig. 2a).

The effectiveness of the assimilation of the cloud-drift wind data apparently varies with TC intensity. For a strong TC (e.g. Sinaku, central pressure 960 hPa, Fig. 2a), the track errors are reduced at all the forecast times. However, for a weak TC (e.g. Fungwong, central pressure 975 hPa, Fig. 2b), the track errors are increased at two forecast times.

If a central pressure of 960hPa is selected as the demarcation between strong and weak TCs, the mean track error changes for the strong TCs show that assimilation of cloud-drift winds gives significant improvements, with track error reductions of 25% and 21% at 24 and 48 h respectively (Fig. 3). However, for weak TCs, slight increases in track errors are observed.

4. Discussion

The results from these 22 cases suggest that track prediction of strong TCs is more sensitive to the upper tropospheric data, which is reasonable since these have a deeper vertical structure than the weak TCs. More case studies are required to ascertain this conclusion. It would also be of interest to examine cases of weak TCs in which lower tropospheric cloud-drift winds are available.

References

Brian, J. S., S. V. Christopher, and E. T. Robert, 2001: The impact of satellite winds on experimental GFDL hurricane model forecasts. *Mon. Wea. Rev.*, **129,** 835-852.

Goerss, J. S., C. S. Velden, and J. D. Hawkins, 1998: The impact of multispectral GOES-8 wind information on Atlantic tropical cyclone forecasts in 1995. Part II: NOGAPS forecasts. *Mon. Wea. Rev.*, **126,** 1219-1227.

Xiao, Q., X Zou, and M Pondeca, 2002: Impact of GMS-5 and GOES-9 satellite-derived winds on the prediction of a NORPEX extratropical cyclone. *Mon. Wea. Rev.*, **130,** 507-528.

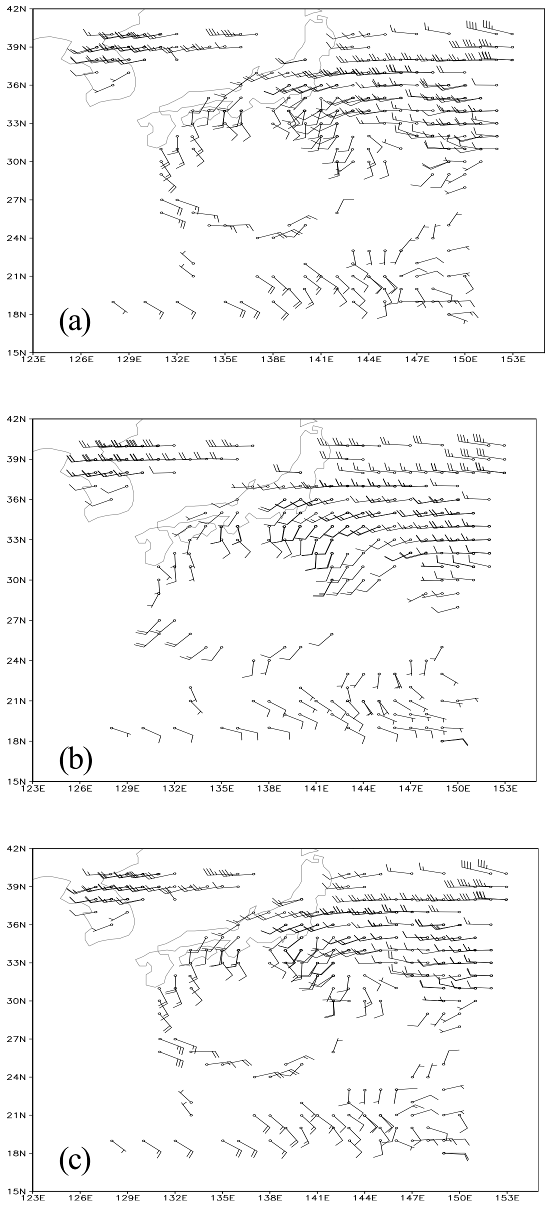

Fig. 1. (a) The cloud drift winds at 1200 UTC 17 August 2002 at 250-300hPa, (b) original analysis and (c) analysis with 4DVAR-assimilated cloud-drift winds.

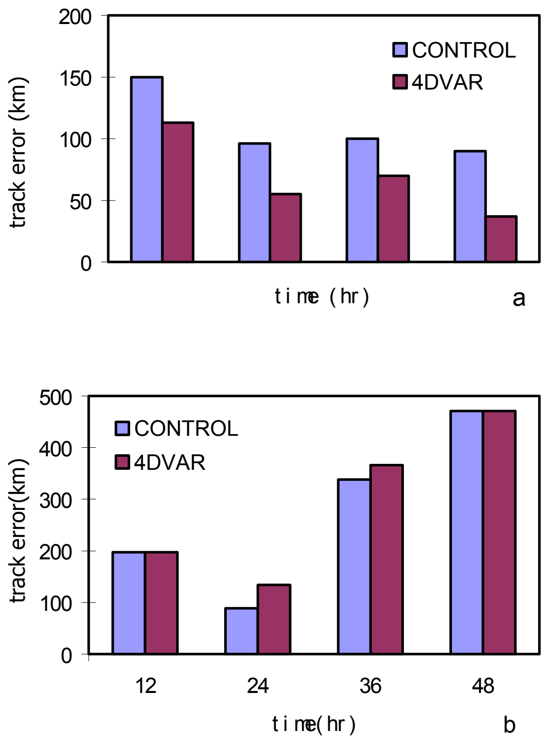

Fig. 2. Track errors from (a) Typhoon Sinlaku at 1200 UTC on 3 Sep 2002, and (b) Tropical Storm Fungwong at 0000 UTC on 25 Jul 2002.

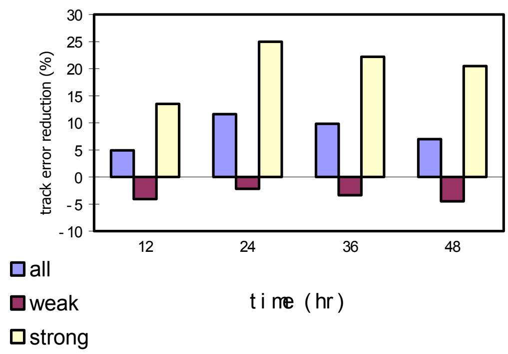

Fig. 3. The mean percentage reduction in track errors due to the assimilation of cloud drift winds for different types of TCs.